

國立交通大學

電機學院與資訊學院 電子與光電學程 碩 士 論 文

高效率光子晶体發光二極体之研究

**A STUDY OF HIGH EFFICIENCY LEDS BY USING
PHOTONIC CRYSTAL TECHNOLOGY**



研 究 生：褚 宏 深

指導教授：郭浩中教授

中華民國95年10月

高效率光子晶体發光二極体之研究

A STUDY OF HIGH EFFICIENCY LEDS BY USING PHOTONIC CRYSTAL TECHNOLOGY

研究生：褚宏深

Student: HungShen Chu

指導教授：郭浩中 教授

Advisor: Prof.HaoChang Kuo

國立交通大學

電機學院與資訊學院專班 電子與光電學程

碩士論文

A Thesis

Submitted to Degree Program of Electrical Engineering and Computer Science

College of Electrical Engineering and Computer Science

National Chiao-Tung University

in Partial Fulfillment of the Requirements

for the Degree of Master

in

Electronics and Electro-Optical Engineering

October 2006

Hsinchu, Taiwan, Republic of China

中華民國95年10月

國立交通大學 研究所碩士班

論文口試委員會審定書


本校電機學院與資訊學院 電子與光電學程研究所碩士班褚宏深君

所提論文 高效率光子晶体發光二極體之研究

A Study of High Efficiency LEDs by Using Photonic Crystal Technology

合於碩士論文資格水準、業經本委員會評審認可。

口試委員：



_____	_____
_____	_____
_____	_____
_____	_____
_____	_____

指導教授：

_____	_____	_____
-------	-------	-------

系主任：

教授

中華民國 95 年 月 日

高效率光子晶体發光二極体之研究

研究生：褚宏深

指導教授：郭浩 中博士

國立交通大學 電機學院與資訊學院 電子與光電學程（研究所）碩士班

摘 要

如何加強 LEDs 的發光效率呢？加強內部量子效率是一個根本的方式，但是這須要從磊晶成長技術著手，要付出相當大的成本。或可以改善級汲光效率為途徑，例如表面粗糙化，較厚的窗戶層，或者以金屬為反射面。在本研討工作，採取光子晶體反射層為提高發光效率的手段。光子晶體反射層採用介電質材料。介電質材料是以電偶極振盪為其光反射機制。因此僅有及微小的能量耗損，是極佳的反光材料。

本研討將比較光子晶體LED與 ITO LED，金屬反射鏡LED 之效能差異。藉此來說明光子晶體LED的優越性。

A STUDY OF HIGH EFFICIENCY LEDs BY USING PHOTONIC CRYSTAL TECHNOLOGY

Student: HungShen Chu

Advisor: Dr. HaoChang Kuo

Degree Program of Electrical Engineering and Computer Science
National Chiao-Tung University

Abstract

How to maximize the efficiency of LEDs? One way is to increase the internal quantum efficiency, this way should put efforts in epitaxy ; the other way is to increase the extraction efficiency .There are many techniques to improve the extraction efficiency, such as rough surface, thick window-layer, wafer bonding with metal reflector...etc. , In this study , we try a new method to increase the light output , that is ,photonic crystal technique . The reflectance ratio of 1dimension photonic crystal reflector is better than metal reflector . It is because the material of PhC layers used for LEDs is dielectrics . The light reflection of dielectrics is dipole-oscillation mechanism , this way, the incident light will not lose energy.

Here we will compare the PhC LED to the ITO LED and Metal reflector LED to convince the advantage of the photonic crystal technology .

誌 謝

感謝指導教授郭浩中老師給我這機會參與研究，並給予啟發性獨立思考與作學問的方法，並給我寶貴的意見與讓我體會到熱心的研究精神，可以在最短的時間內完成研究實驗使我受益良多，感謝郭老師實驗室與我接觸過的同學也幫助我很多，在電資專班修課的過程中感謝跟我一起成長奮鬥過的同學，我們曾經利用下班空閒時間努力與討論解決課業上問題。使我這兩年進修過程中讓自己深深感覺到真正的「創意」和「突破」。



CONTENTS

中文摘要	i
Abstract	ii
誌謝	iii
Contents	iv
List of Tables	x
List of Figures.....	xii
Chapter 1 Introduction	1
1.1 MOTIVATION.....	1
Chapter 2 Material, Electrical and Optical Properties of III-Nitrides.....	8
2.1 MATERIAL PROPERTIES	8
2.2 ELECTRICAL PROPERTIES.....	10
2.3 OPTICAL PROPERTIES.....	13
Chapter 3 Theory of Emission Efficiency Improvement	16
3.1 BASIC CONCEPTS OF PHOTONIC CRYSTALS.....	16
3.2 PHYSICS OF 1D PHOTONIC CRYSTAL S	18
3.3 PHOTONIC CRYSTALS- ADVANCED APPROACH IN ENHANCING OPTICAL EXTRACTION ...	21

Chapter 4 Device Fabrication and Processing	27
4.1 COMPOUND SEMICONDUCTOR MATERIALS	27
4.2 EPITAXY	28
4.3 GAN LEDs DEVICE PROCESS	31
4.4 FABRICATIONPROCESS OF 1D PhC LED	32
4.5 EXPERIMENTAL DESIGN S OF 1D PhC LED	38
Chapter 5 Experimental Results	45
5.1 LIGHT EMISSION MAPPING RESULTS OF HALF-CUT WAFERS	46
5.2 AXIAL EMISSION MEASUREMENT IN LAMP-FORM	56
5.3 RADIOMETRIC AND PHOTOMETRIC MEASUREMENT OF NiAu,ITO AND PC LED IN LAMP-FORM	58
5.4 RADIATION PATTERN OF NiAu,ITO AND PC LED PACKAGED IN TO CAN	60
Chapter 6 Conclusions and Future Works	64
Reference	R1
Appendix 1 - Estimate of the fraction of light extracted from GaN LED.....	R4

LIST OF TABLES

Table 4.1 Mask List	32
Table 4.2 1d PC LEDs chip process:	35
Table 4.1 Simulation: 1D-PhC structure – α of blue LED:	38
Table 4.2.Simulation: 1D-PhC structure – β of green LED	39
Table 5.1 Light Emission Mapping Result of Half Cut Samples.....	46
Table 5.2 Axial Emission Intensity Measurement of PC & ITO LEDs Lamps.....	57
Table 6.1 Estimation of Light LOP from Top and Bottom of LED	64



LIST OF FIGURES

Fig. 1.1 Internal reflection and photons trapping in LED	2
Fig. 1.2 Structure of Top emitting LED	3
Fig. 1.3 Structure of Flip Chip LED	4
Fig. 1.4 The geometric structure of photonic crystal in dielectrics	6
Fig. 2.1. Physical and chemical properties of binary nitride semiconductors	7
Fig. 3.1 : Band Structure of hexagonal lattice of holes	16
Fig. 3.2 Calculated photonic bandgap structure.	19
Fig. 3.3 Possible paths of emitted light in GaN based LED structure.....	20
Fig. 3.4 The 2D-PhC convert the guided mode to the radiation mode into air	21
Fig. 3.5.Top emitting LED using PhC technology	23
Fig. 3.6 Flip chip LED structure using PhC technology.....	23
Fig. 4.1 A plot of energy bandgap and lattice constant for major III-V compounds ..	27
Fig. 4.2 . Simulation: reflection spectrum for 1D-PhC for blue LED	31
Fig..4.3 .Simulation: reflection spectrum for green LED	32
Fig. 5.1 LOP Distribution of #01-301C w and w/o PhC structure	48
Fig. 5.2 Raw data of LOP Distribution of #01-301C w and w/o PhC structure	49
Fig. 5.3 LOP Distribution of #02-301A w and w/o PhC structure.....	50
Fig. 5.4 Raw data of LOP Distribution of #02-301A w and w/o PhC structure	51

Fig. 5.5 LOP Distribution of #03-301D w and w/o PhC structure.....	52
Fig. 5.6 Raw data of LOP Distribution of #03-301D w and w/o PhC structure	53
Fig. 5.7 LOP Distribution of #04-2882A w and w/o PhC structure.....	54
Fig. 5.8 Raw data of LOP Distribution of #04-2882A w and w/o PhC structure	55
Fig. 5.9 LI Curve of PC and ITO LED Lamps	57
Fig.5.10 Radiation pattern of Blue LED w and w/o PC structure.....	60
Fig.5.11 Raw data of radiation pattern of Blue LED without PC structure.....	61
Fig.5.12 Raw data of radiation pattern of Blue LED with PC structure.....	61
Fig.5.13 Radiation pattern of Blue LED w and w/o PC structure.....	62
Fig.5.14 Radiation pattern of ITO and NiAu LED w and w/o PC structure.....	63



Chapter 1. Introduction

1.1 Motivation

There is a strong demand to improve the luminous efficiency and brightness of light emitting diodes. It is necessary to efficiently transform electrical energy into light and extract it from devices. Up to date, the Wall Plug Efficiency (Optical Power out/Electrical power in (%)) for blue LED is about 7%. In general two methods have been approached to raise the LED efficiency: improving the generation efficiency of the light inside the device, i.e internal quantum efficiency; and improving the extraction efficiency of the light from the device, i.e optical extraction efficiency and external quantum yield.



The internal quantum efficiency can be improved mainly in the epitaxial growth stage, and extensive works have been carried out and remarkable results have been achieved in this field. However, the optical extraction efficiency remains low since the materials used in the LEDs generally have high refractive indices that trap the light inside the device as a result of an internal reflection. This can be explained by using Fig.1.1.

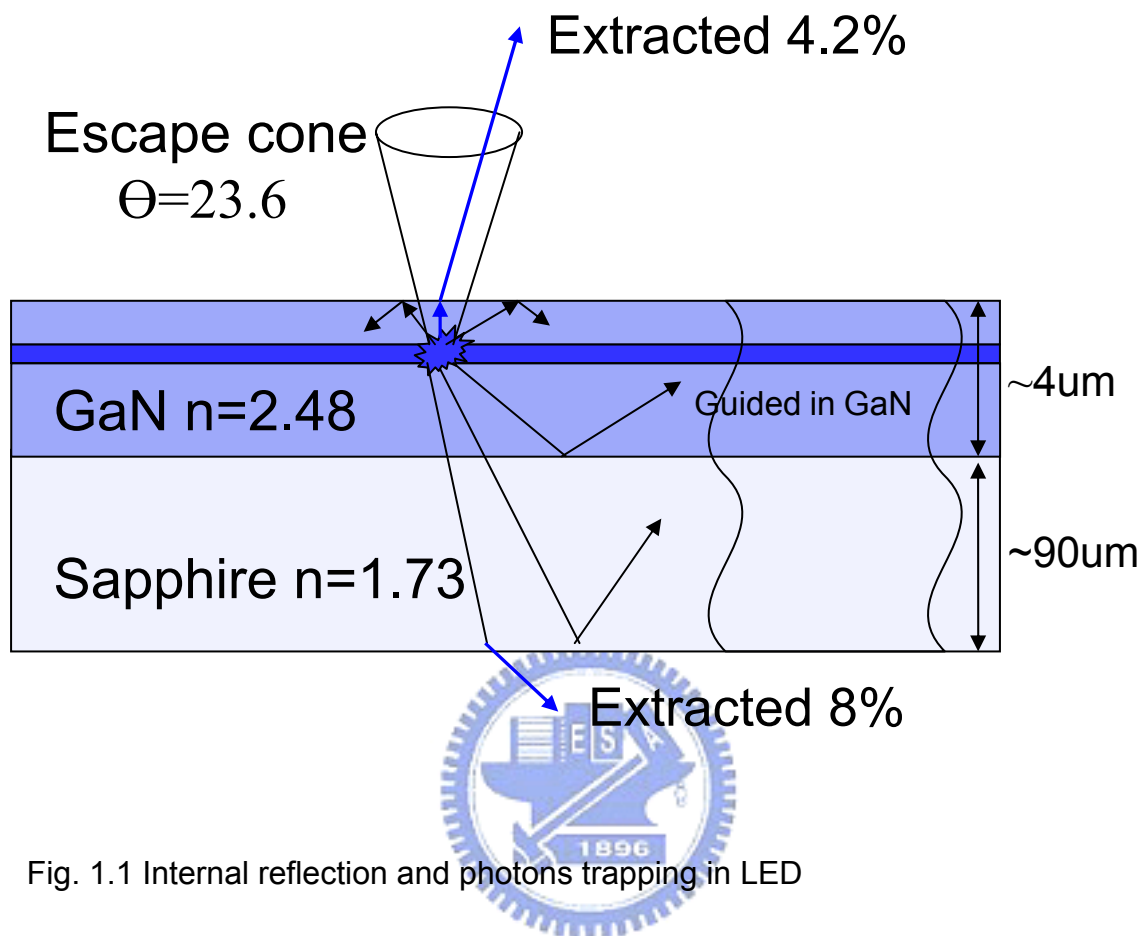
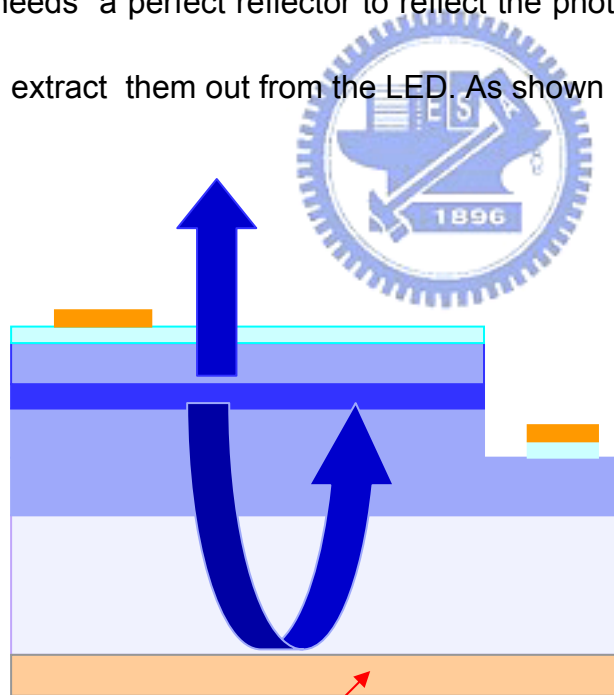


Fig. 1.1 Internal reflection and photons trapping in LED

As seen from the schematic drawings shown in Fig.1.1, the light is trapped due to high refractive index ($n=2.48$) of GaN and reflects many times between top and bottom of the GaN layer. Only about $1/4n^2$ of the light radiate through top and bottom, the extraction efficiency is less than 10%, more than 66% photons are trapped in LED materials. Therefore, any way of destroying parallelism of the GaN layer – etching, lapping, polishing or texturing – will help to extract this light before it is absorbed in GaN.

Some famous companies such as Lumiled, Cree, Osram and some Taiwan LED manufactures have their own technology strategic to improve the optical extraction efficiency, such as making LED on patterned substrates, using under-cut side wall structure, using surface roughness using and photonic band gap structure to enlarge the photon escape cone. These companies also developed their IPs to protect above mentioned technologies.

In the blue LED structure design both for top emitting and Flip chip structure, it always needs a perfect reflector to reflect the photons upward to the top surface in order to extract them out from the LED. As shown in Fig. 1.2. ; Fig. 1.3.



Perfect reflector

Fig.1.2 Structure of Top emitting LED

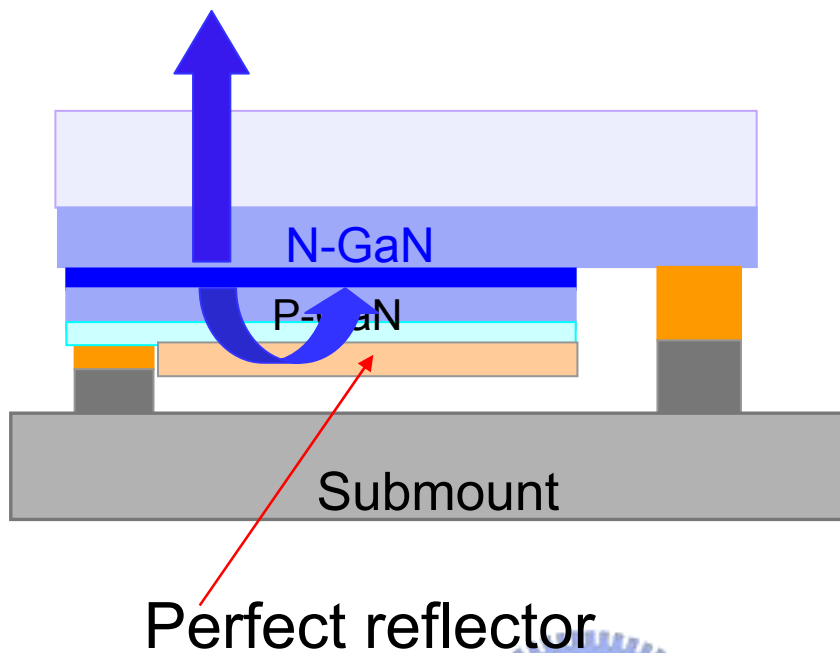


Fig.1.3 Structure of Flip Chip LED



The said 'perfect reflector' here means lossless reflector . If the reflector is a metal reflector , then the reflection loss should be higher than dielectric reflector . The reflection mechanism of dielectrics is mostly dipole vibration at same frequency of incident ray. As for the metal reflector, it will loss some energy to the free carriers from the incident light. . Basically, the most important property to LEDs is the light emission ability . The emission ability depends on the internal quantum efficiency and extraction efficiency . The internal quantum efficiency is attributed to Epitaxy quality ; the extraction efficiency degree come from device structure design and chip process .

The reflector is a very effective tool to increase the light extraction . According to mentioned previously , we know the dielectric reflector is better than the metal reflector. And the materials of photonic crystal structure used in LEDs is dielectrics , although the essential definition of photonic crystal never limits its material should be dielectrics .Now let us introduce photonic crystal briefly .

Photonic crystals are periodic dielectric or metallo-dielectric (nano) structures that designed to affect the propagation of electromagnetic (EM)waves in the same way as the periodic potential in a semiconductor crystal affects the electron motion by defining allowed and forbidden electronic energy bands. The absence of the propagating EM modes inside the structure , in a range of wavelengths called a photonic band gap, gives rise to distinct optical phenomena such as inhibition of spontaneous emission high-reflecting omnidirectional mirrors and low-loss wave guiding among others.

Since the basic physical phenomenon is based on diffraction , the periodicity of the photonic crystal structure has to the same length-scale as half the wavelength of the EM waves . i.e., ~300 nm for photonic crystals operating in the visible part of the spectrum.

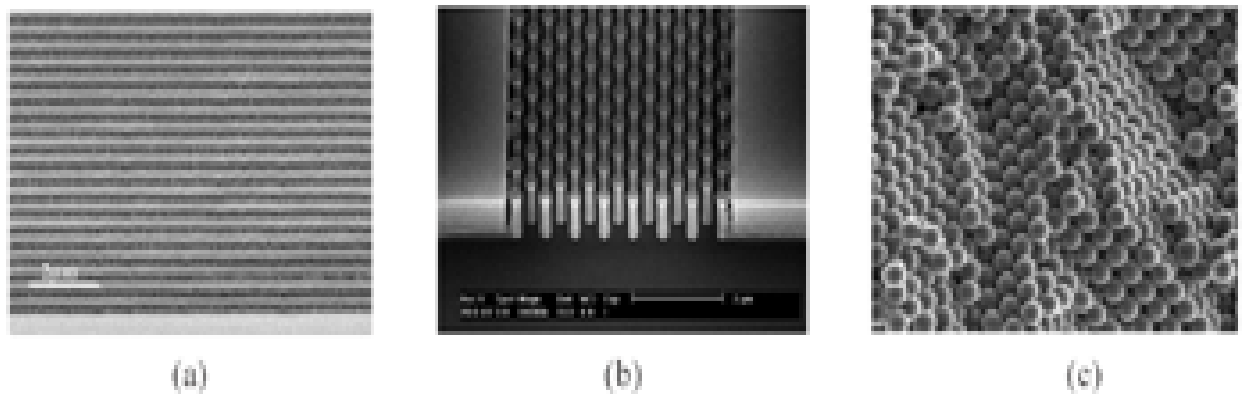


Fig.1-4 The geometric structure of photonic crystal in dielectrics

(a) 1D PhC , (2) 2D PhC , (c) 3D PhC

Figure 1-4 shows the schematic depiction of photonic crystal periodic in one , two, and three directions , where the periodicity is in the material (typically dielectric) structure of the crystal .

One dimensional photonic crystal (1D PhC) consists of alternating layers of two dielectric media of refractive indices n_1 and n_2 . Almost all the 1D-PhC structure can form a complete photonic bandgap .

Similar to electronic bandgap, no photon frequencies in the gap region of the photonic crystal correspond to the allowed state for this medium. Hence, the photons in this frequency range cannot propagate through the photonic crystal due to the photons of these frequencies are multiply scattered by the scattering potential produced by the large refractive index contrast n_1/n_2 . In other words, of photons of

frequencies corresponding to the bandgap region are incident on the 1D-PhC structure, they will be reflected from the surface of the 1D-PhC structure and will not enter the crystal. Further more, this kind of reflection is independent on the incident angle and polarization of the incident photons. So 1D-PhC structure can act as a perfect reflect mirror with omnidirectional, high reflection (100%). We can use 1D-PhC as a perfect mirror in high efficient LED structure design.



Chapter 2.

Physical , Electrical and Optical Properties of III-Nitrides

2.1 Materials properties

The alloy system Al–Ga–In–N, when grown in the typical wurtzite structure, forms a continuous and direct band-gap alloy from 6.2 eV (AlN) to 0.8 eV (InN), with GaN itself possessing a large band gap of 3.4 eV. Linked to the enormous differences in the band gap of the binary crystals, also the bond energy between the metal and nitrogen atoms in the crystal lattice show large variations, with $EB(\text{Al–N})=2.88$ eV, $EB(\text{Ga–N})=2.2$ eV and $EB(\text{In–N})=1.93$ eV in the binary nitrides AlN, GaN and InN. Consequently, the group-III nitrides also differ enormously in their thermal stability, with AlN and GaN exhibiting melting points of about 3200°C and 2500°C, respectively, while InN already sublimates at temperatures above 550°C (Fig.2.1) . For this reason, (Al, Ga)N films are typically grown at temperatures above 1000°C, whereas the deposition of indium containing alloys is performed at temperatures below 800°C. Furthermore, the lattice mismatch between AlN and GaN is about 3.5%, the lattice mismatch between GaN and InN is as high as 10%. As illustrated in Fig. 2.1[1], the chemical and physical properties of the group-III nitrides are much more diverse than

the properties of the corresponding arsenide (or phosphide). The profound differences in the properties not only affect the crystal growth, but also the gas-phase chemistry in the MOCVD growth chamber[2].

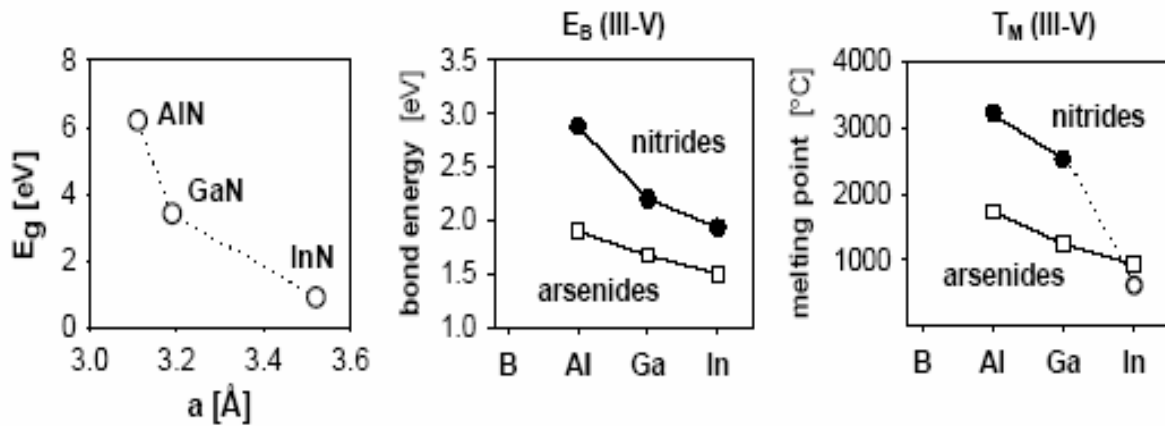


Fig.2.1. Physical and chemical properties of binary nitride semiconductors:

left: band gap energy E_g as a function of lattice parameter a ,

center : comparison of binary bond energies for group-III nitrides and arsenides,

right: comparison of the melting points of binary group-III nitrides and arsenides.

Although under investigation for several years, the device design opportunities offered by the alloy system Al–Ga–In–N have not yet been fully explored. Similar to the band gap of InN, a variety of properties of the group-III nitrides remain unclear. These discrepancies can often be attributed to the insufficient quality of the investigated material. Advances in the reactor design, the availability of AlN, GaN or alloy substrates, and possibly the development of alternative precursors will lead to improvements in the quality of the epitaxial layers. Flow modulation epitaxial

processes and digital alloy approaches may gain importance in particular for the growth of alloys containing both AlN and InN. The influence of kinetic effects on miscibility and ordering needs further investigation as well. Efforts to take advantage of the polarization effects in group-III nitrides, particularly for doping purposes, are just in the early stages of development. Further concerted efforts are necessary to meet these challenges in the materials growth and the understanding of the group-III nitrides.

2.2 Electrical Properties



Because gallium nitride (GaN) is an attractive material which has a wide direct band gap, GaN-based optoelectronic devices such as light emitting diodes (LEDs) and laser diodes (LDs) in blue and ultraviolet wavelength regions have been intensively researched and are also commercially available. [3]

In the GaN-based LED fabrication, the p-contact is generally formed by depositing metal layers on p-GaN located at the top of GaN-based LED quantum well structure. Due to the high contact resistance to p-GaN originated from low doping density of p-GaN, many studies have been made to improve the poor electrical

performance. Among these are the use of multilayer materials such as Ni/Au and Ta/Ti and the use of additive metal outline to increase the electron spreading area of p-GaN, etc. [4–7]. In general, Ni/Au ohmic contacts to p-GaN are widely studied in commercial GaN LEDs.

These metal contacts, however, are only partially transparent and most of the light generated in the LED cannot be emitted through the top of the devices even though the GaN-based LEDs are optically transparent. If the ohmic contacts could be formed by transparent conductive oxides instead of partially transparent multilayer metals, the light emitting area can be increased so that light with a higher intensity could be obtainable, therefore, more efficient LEDs can be fabricated without the loss of contact area. However, up to today, only a few experiments on transparent conductive oxides have been carried out as the materials for ohmic contact to GaN-based LEDs.

ITO is a well known transparent conducting material with resistivity in the range of low $10^{-4} \Omega\text{cm}^2$ and with transmittance higher than 90% in the blue wavelength region at optimized conditions[7]. Therefore, ITO has been widely applied in various optoelectronic devices. In this study, ITO contact properties were studied by depositing ITO on p-GaN to investigate a possibility of forming transparent ohmic contact on p- GaN. Because the substrate pre-treatment before the contact formation is one of the most important factors in forming a good ohmic contact, the effect of

substrate pre-treatment on the ITO contact properties was also investigated.

Electrical properties of ITO contact on p-GaN have been investigated as a function of different surface treatments to p-GaN, annealing temperature, and annealing time. The contact resistance initially decreased with the increase of annealing time and showed a minimum contact resistance at a certain annealing time and temperature. Also, the surface treatment before ITO deposition affected the contact resistance.

ITO contact resistivity in the range of low $10^{-1} \Omega\text{cm}^2$ could be obtained for certain conditions such as the surface treatment B (Acetone+ Alcohol+ HCl+ 3HCl:HNO₃+(NH₄)₂S) followed by the annealing at 600°C for 90 s and the surface treatment C (Acetone+Alcohol+HCl+3HCl:HNO₃+KOH+(NH₄)₂S) followed by the annealing at 700°C for 60 s, etc. The $I-V$ characteristic of the deposited ITO contact was initially Schottky contact, however, at the optimized annealing conditions, the $I-V$ curve showed a near-ohmic behavior possibly due to the formation of a mixed interface layer. Optical transmittance of the 100 nm ITO contact annealed at 600°C for more than 90 s was higher than 90% while that of 50 nm Ni/50 nm Au, typically used for the contact on p-GaN, is lower than 40%. Therefore, it is believed that if the ITO contact to p-GaN is formed after a proper surface treatment followed by adequate annealing, the ITO contact could be applicable as a transparent contact to p-GaN.

2.3 Optical Properties

GaN-BASED light-emitting diodes (LEDs) have been the subject of extensive investigations, and have been developed because of their potential applications in areas such as full color displays, full-color indicators, and high-efficiency lamps [10]–[17]. However, the GaN-based LED has a critical weakness in that its fabrication mainly involves the use of the lateral carrier injection type due to the absence of an appropriate conducting substrate. In this case, a current crowding problem is often encountered and impedes the development of the efficient GaN based LEDs. Several groups have reported on studies relating to this issue, both theoretically and experimentally [18]–[20]. Based on the assumption that the transparent electrode represents a perfect current spreader, Eliashevich *et al.* reported that the conductivity of an n-type GaN layer has a profound effect on uniform current spreading [18]. It has been shown that the uniform current spreading is essentially attained above the critical n-type carrier concentration. However, a thin metal film has a much higher sheet resistance than its corresponding bulk material due to the reflection of conduction-electrons from defects that are trapped in the film during the deposition and from internal surfaces [21]. Therefore, the resistivity of the transparent electrode should not be ignored in the development of a more accurate

model. Based on this consideration, more highly developed theoretical model has recently been proposed and important parameters such as the current density, the resistivities of the transparent electrode and n-type layers, and the effective length for the lateral current path were found to be important factors in uniform current spreading [9], [19].[20]

From the standpoint of both uniform current spreading and high extraction efficiency of a generated light, the determination of the proper thickness of the transparent electrode becomes very important. However, no systematic study on the transparent electrode has yet been reported because of a lack of understanding of the relationships between the transparent electrode and the n-type layer with respect to current spreading. In this study, we report on a method for determining the critical transparent- electrode thickness for the realization of highly efficient LEDs.

Based on the effective length factor, which involves device geometry, significant improvements in LED characteristics have also been demonstrated by local modification of the p-type pad (electrode) geometry [19], [20]. In addition, although it does not mainly concern the current spreading problem, the geometrical design such as the interconnected micro disk LED also showed a 60% increase in optical emission efficiency compared to the conventional broad-area LED [22]. These results indicate the importance of geometrical design on device efficiency. In this regard, in terms of the ideal geometrical design, which gives perfectly uniform current spreading

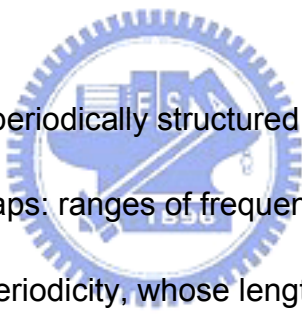
conditions, we report on an attempt to realize highly efficient GaN-based LEDs in the absence of a transparent electrode.

Based on the current spreading phenomenon in the GaN based LEDs, promising fabrication method and design rules were investigated. It was possible to maximize the device performance from the determination of the critical transparent-electrode thickness during the fabrication process. For this work, first, the resistance of the n-type layer should be minimized in order to maximize the carrier injection into the n-type layer. The critical transparent-electrode thickness should then be determined according to the relation of R_{sh} , resulting in the maximization of the carrier injection into the p-type layer through the transparent electrode. This result will be very useful for the fabrication of highly efficient devices in the conventional LED process. In addition, we also investigated the geometrical design rule for the highly efficient LED in terms of a perfect current spreading. Based on this consideration, it was even possible to realize the ideal LED geometry without the need for a transparent electrode, which resulted in improvement in LED performances, compared with a conventional LED. Finally, it is concluded that, although the determination of the critical transparent-electrode thickness has a great influence on the device performance, the design of ideal geometry is a better method to fabricate the highly efficient LED considering the extremely improved device performance as well as the simple fabrication process.

Chapter 3.

Theory of Emission Efficiency Improvement

3.1 Basic Concepts of Photonic Crystals



Photonic crystals are periodically structured electromagnetic media, generally possessing photonic band gaps: ranges of frequency in which light cannot propagate through the structure. This periodicity, whose length scale is proportional to the wavelength of light in the band gap, is the electromagnetic analogue of a crystalline atomic lattice, where the latter acts on the electron wave function to produce the familiar band gaps, semiconductors, and so on, of solid-state physics.

Photonic crystals represent a class of nanomaterials in which alternating domains of higher and lower refracting indices produce an ordered structure with periodicity on the order of wavelength of light..

In a photonic crystal , for certain range if photons and certain wave vectors (that is , direction of propagation), light is not allowed to propagate through this

medium. If we generate light inside, it cannot propagate in this direction. If we send light from outside, it is reflected.

In the case of a large refractive index contrast (defined by the ratio n_1/n_2) photonic crystal with a proper shape of building blocks (domains) and proper crystal symmetry, a complete bandgap develops. In this case, the bandgap is not dependent on the direction of wave vector ,which defines the light propagation ; also, the density of photon states goes to zero in the bandgap region. These materials with a complete gap are often called photonic bandgap materials.

Here we would describe the concept of complete and incomplete photonic bandgap more clearly . A complete photonic band gap is a range of ω in which there are no propagating (real k) solutions of Maxwell's equations for any k , surrounded by propagating states above and below the gap. There are also incomplete gaps, which only exist over a subset of all possible wave vectors, polarizations, and/or symmetries.

3.2 Physics of 1-dim Photonic Crystal

Photonic bandgap crystals are periodic structures in which light is prohibited from having extended modes by classical electromagnetic theory. In practice, these are man-made structures, usually made out of two or more materials with different dielectric constants. The size of the crystal features can be scaled with the wavelength of electromagnetic radiation used due to the linearity of the Maxwell Equations. Typically the unit cell of such a crystal has dimensions which are comparable to the wavelength of radiation it is designed to work with.

The simplest example of a one dimensional photonic crystal is the well known Bragg mirror. A stack of layers of two materials with different dielectric constants and optical thicknesses equal to one quarter of a wavelength each will act as a mirror for light near normal incidence. One way of thinking about this is that there are reflections from each material interface, and those which reflect back constructively interfere, while those which reflect an even number of times destructively interfere, resulting in net reflectivity. In an *infinite* stack of layers, light cannot propagate normal to the interfaces within a specific frequency range. In a finite stack, light incident upon the

stack at near normal incidence will partially reflect. Within the quarter wave stack, the intensity will decay exponentially.

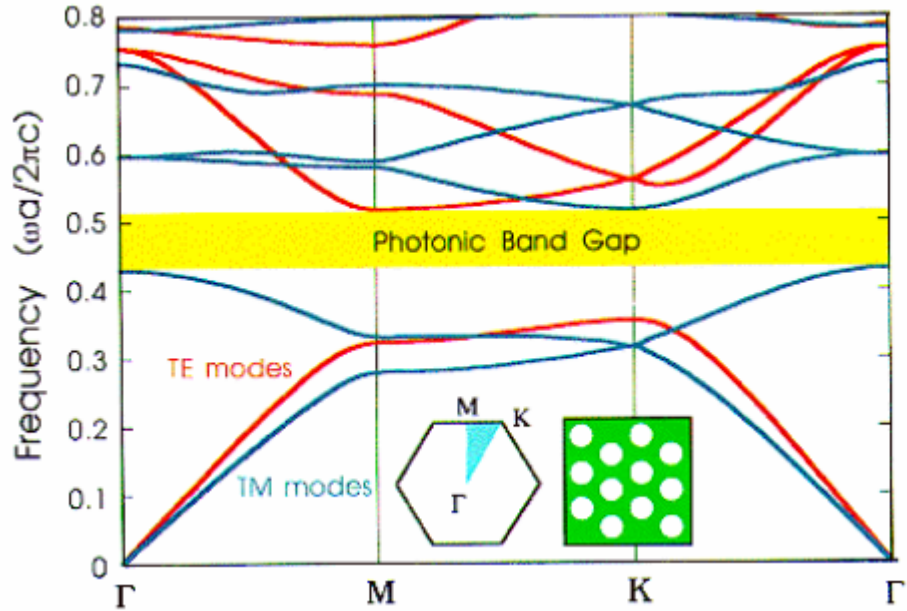


Figure .3.1 : Band Structure of hexagonal lattice of holes

The concept of a Bragg reflector can be extended to two or three dimensions by considering structures with periodicity in more than one direction. In order for such a structure to display a useful bandgap, there must be a frequency range in which electromagnetic radiation cannot propagate in any direction in two or three dimensions. Calculations have revealed that there are many structures which have two dimensional photonic bandgaps [23,27], but fewer that possess a full three dimensional gap [23, 26].

It is sometimes useful to consider a multidimensional photonic crystal as a superposition of several one dimensional crystals at different angles. In this sense, the “Bragg planes” of the crystal can be described as the planes normal to which light is

strongly reflected. In this view, it is clear why it becomes harder to create a photonic crystal in higher numbers of dimensions, as it becomes more difficult to find a lattice which provides reflecting Bragg planes in all directions.

In these experiments, we will be concerned with a photonic crystal made by drilling (or etching) a hexagonal array of air holes into a slab of dielectric material. The band structure for this crystal is shown in figure 3.1. It can have a complete two dimensional bandgap for both possible polarizations in the lattice. We will be designing these structures for use with optical and infrared radiation, which results in hole spacings (lattice constants) on the order of hundreds of nanometers in materials with an index of refraction around 3.2.

There is another class of photonic crystals made using combinations of dielectric materials and metals. These also exhibit very large photonic bandgaps in two and three dimensions [28]. At microwave frequencies, these structures are very useful, but most metals are too lossy at optical frequencies to be useful in high Q cavities. Therefore, we will restrict discussion to dielectric photonic crystals.

3.3 Photonic crystal---- Advanced approach in enhancing optical extraction

Features of Photonic Crystals

Spontaneous emission arises from the intricate interplay between a radiating system and its surrounding environment. A prominent example of this interplay can be seen in a photonic crystal, where spontaneous emission can be enhanced, attenuated or even suppressed by changing the density of electromagnetic states at the transition frequency, or by changing the orbital angular momentum of the emitted photon. The ability to control spontaneous emission could have profound consequences on many optoelectronic devices. One device that could potentially benefit from this control is the LED, which spontaneously emits radiation from a p-n junction. In the past thirty years, various approaches have been proposed to enhance the extraction efficiency of LEDs. Many of these approaches rely on clever geometrical optical designs to either enlarge the escape cone of photons using a hemispherical dome, or to enable multiple entries of photons into the escape cone using photon recycling or surface roughness. These approaches, however, do not alter directly the spontaneous emission properties of the devices.

Photonic crystals are ordered nanostructures in which two media with different refractive indices are arranged in periodic form. In the case of a large refractive index

contrast photonic crystal with proper shape of building blocks (domains) and proper crystal symmetry, a complete photonic bandgap develops. As shown in Fig.3.2.

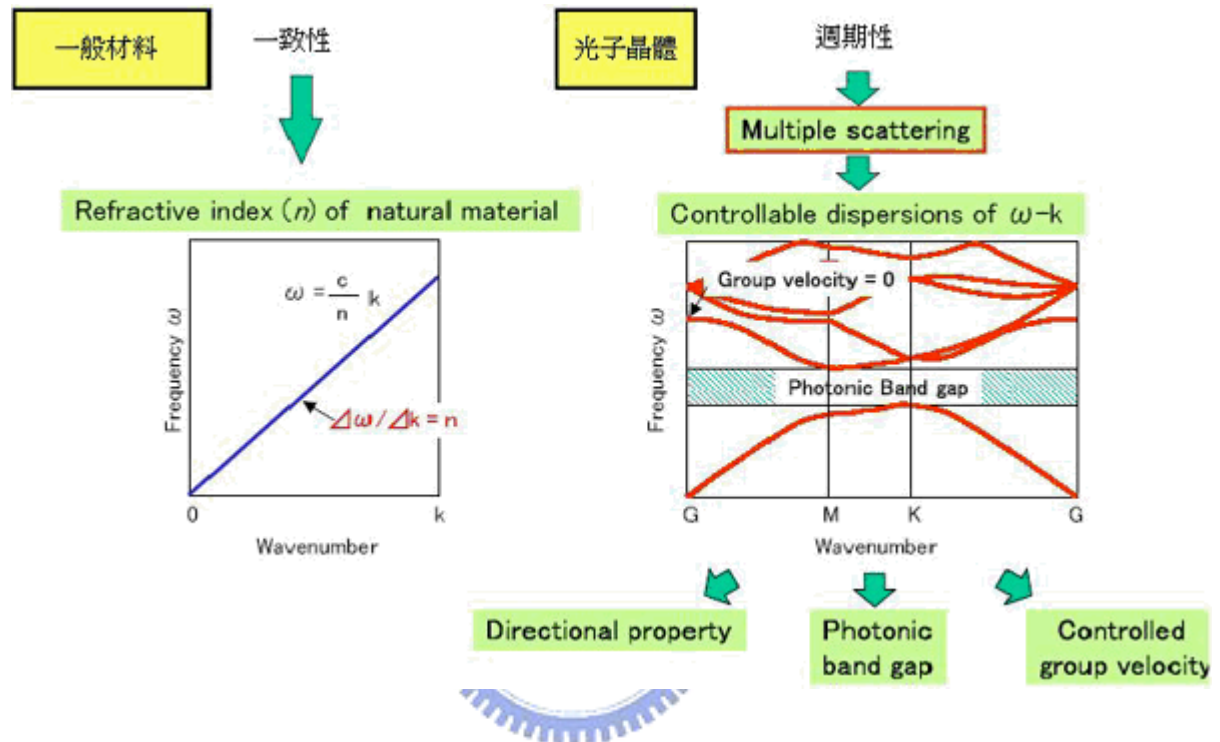


Fig.3.2 Photonic bandgap structure.

For the application of photonic crystal technology in LEDs to improve the optical extraction efficiency, two schemes can be considered for PhC assisted LEDs: formation of bandgaps to prevent emission into guided modes, or PhC acting as diffraction gratings to extract guided light.

Let us first consider the various paths accessible to light emitted in a classic GaN LED (Fig.3.3): 6% of the light is emitted in air towards the top (assuming a transparent contact), which can be doubled if a mirror is placed under the sapphire

substrate. 22% is trapped by TIR but can propagate in the sapphire – we call this fraction the substrate light. Finally, 66% is trapped in the GaN layer by TIR at the air and sapphire interfaces. We label this light as guided light. Substrate light has negligible interaction with the PhC region, as it propagates for long distances in the thick (~100 μm) transparent sapphire wafer, and impinges on the PhC no more than once before exiting the LED region. Therefore, the PhC only aims at extracting guided light.

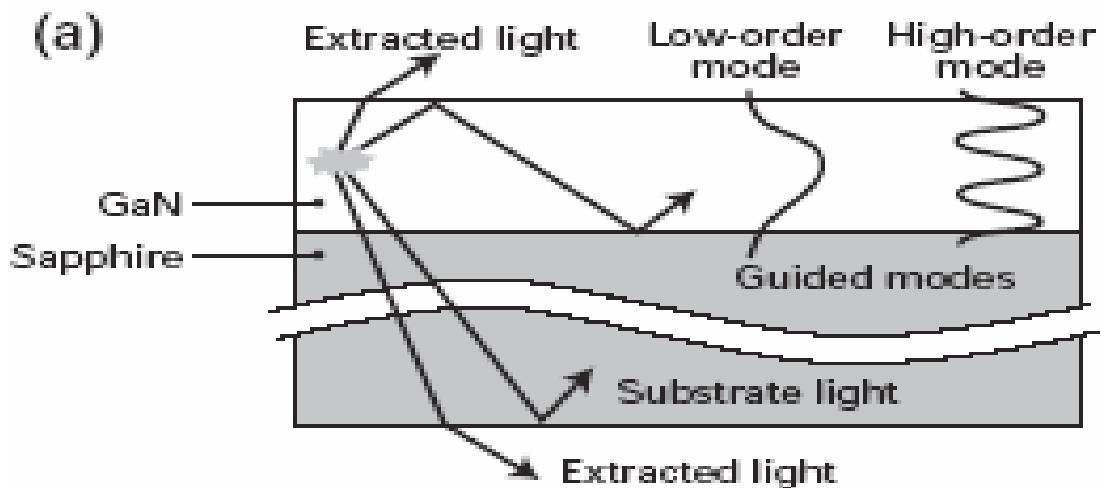


Fig.3.3 Possible paths of emitted light in GaN based LED structure.

The 2D photonic crystal can act as diffraction gratings in extracting light in GaN-based LEDs. Many research works have been carried out to study and characterize a solution based on tailoring the structure of guided modes which

enables nearly all of the guided light to be prone to interaction with the PhC. This can be illustrated by Fig. 3.4.

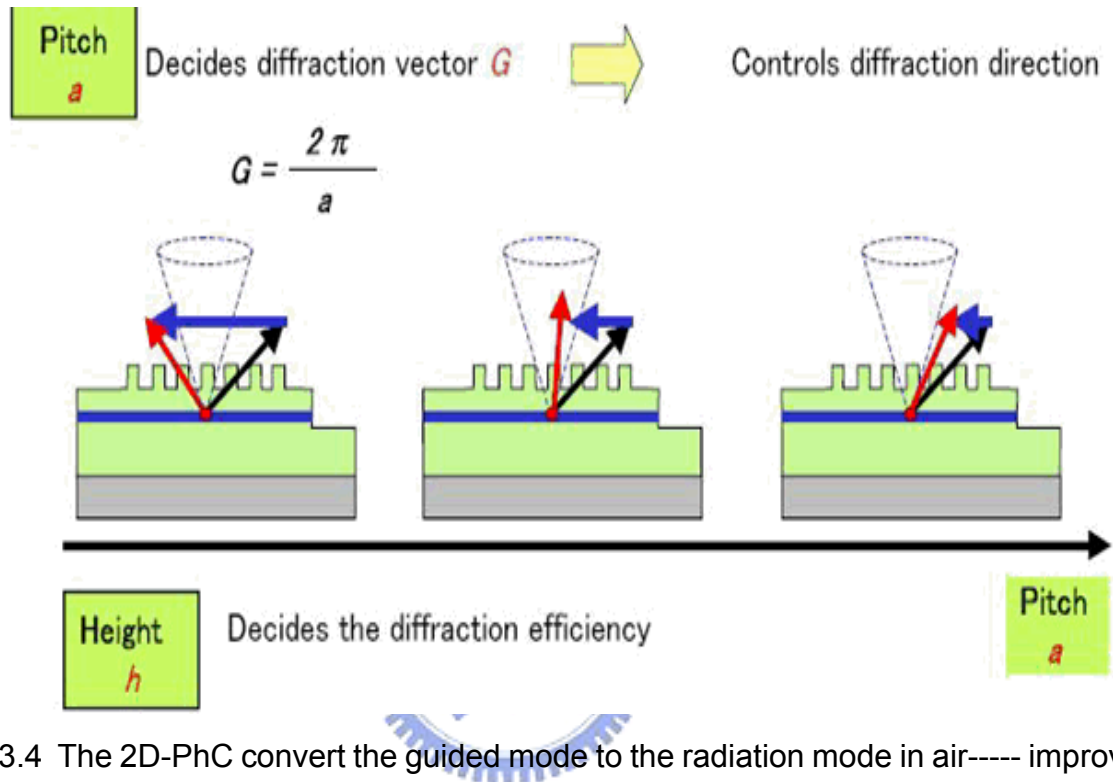


Fig.3.4 The 2D-PhC convert the guided mode to the radiation mode in air----- improve the light extraction efficiency

Problems exists in PhC-LED

However, for the fabricated LEDs using photonic crystal technology, it is still far from an optimal design, a lot of work need to be done to confirm the validity of the approach of modes tailoring. This improvement comes at no cost or additional fabrication steps, and could easily be combined with future optimisation of the intrinsic PhC properties, bringing us closer to ultra-efficient PhC-assisted LEDs. However,

nonradiative carrier recombination and surface recombination are increased near the etched interfaces. This can pose a problem when the lattice constant of the photonic crystal becomes comparable to the carrier diffusion length in the active region. It is therefore important to avoid penetrating the active region with the photonic crystal. While photonic crystals in general

Result in far-field patterns different from flat-surface rectangular parallelepiped LEDs, other surface structuring techniques maintain the Lambertian emission pattern .

Comparing of 1D-PhC with Al mirror and DBR

Al mirror is a commonly used reflector in LED structure design. But the reflection of Al mirror is not higher than 85% due the metal absorption in the short wavelength region. For DBR structure, its reflection is higher (90%) but is strongly dependent on the incident angle and the polarization of the incident photons. 1D-PhC structure has better reflection properties as compared with Al mirror and DBR structure.

technology solution for 1D-PhC LED

A. For different wavelength, optimize different 1D-PhC structure (*photonic bandgap*) to get maximum reflection.

B. Not only focus on power/brightness enhancement, but also design the far field radiation pattern for different applications.

Our team has proposed several LED structures using 1D-PhC and 1D-PhC to enhance the optical extraction efficiency, as shown in Fig.3.5.,

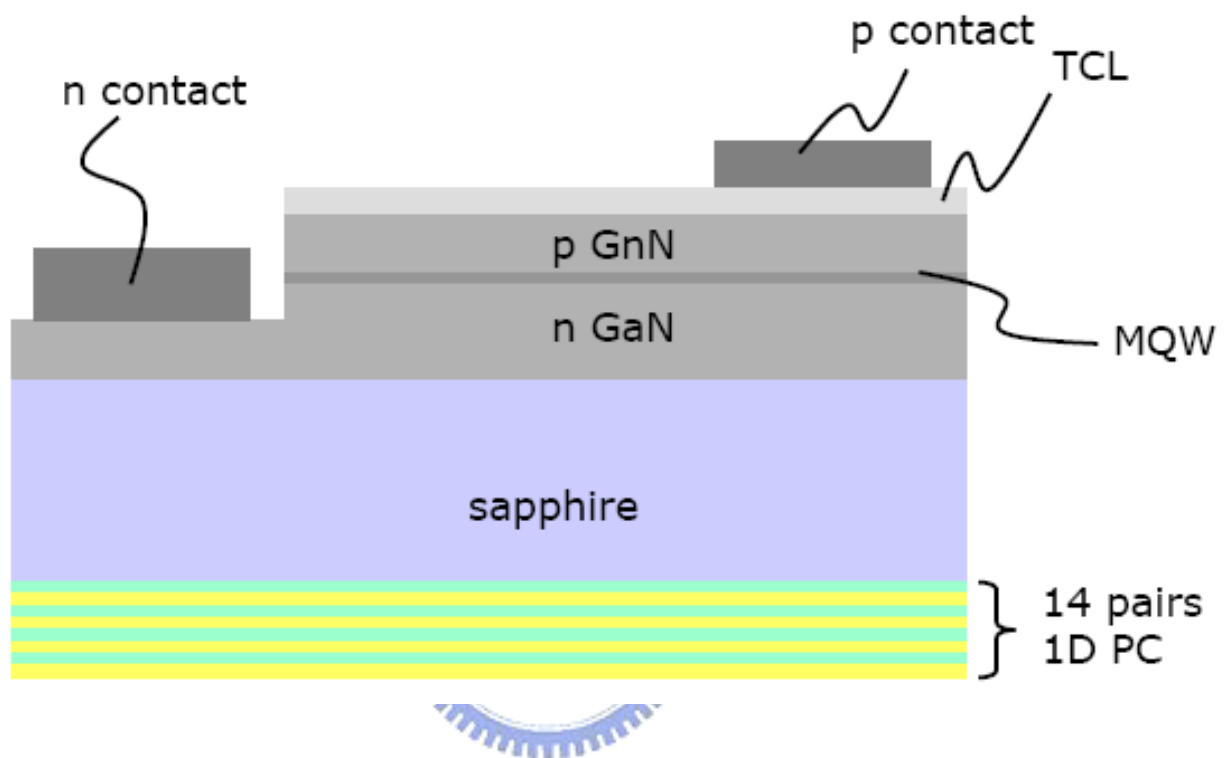


Fig.3.5.Top emitting LED using PhC technology

Chapter 4.

Device Fabrication and Processing

4.1. Compound Semiconductor Materials

Some of the fundamental principles of semiconductor growth mechanisms and the associated practical methods used in the manufacture of wafers for device fabrication are discussed in this section.

Compound semiconductor materials can be realized by the formation of “solid solutions” of two or more starting materials. These solutions occur when atoms of a different element are able to substitute a given constituent of a material without altering its crystal structure. The ability to do so by the new atom is referred to as its miscibility. In order that atoms can form solid solutions over large ranges of miscibility, they must satisfy the Hume Rothery rules:

- They must belong to the same **group** of the periodic table
- They must have comparable **atomic diameters** allowing substitution without large mechanical distortion
- Their **ionicity** must not be very different so as not to affect the tendency to attract / repel electrons from the site by a large amount
- The **crystal structure** of each constituent must be the same

A two component alloy is known as a *binary* alloy; some common examples include GaAs, AlAs, GaP, InP and InAs all of which have the Zincblende (diamond) crystal structure. Similarly a *ternary* alloy is one with three components and a *quaternary* alloy is one with four.

4.2 Epitaxy

Epitaxy refers to the ordered growth of one crystal upon another crystal [97]. Because of the large range of possible semiconductor compounds and their alloys, it is rare in device fabrication to grow bulk crystals of all these materials. Instead, it is more attractive to realize the wider range of materials by epitaxial growth. This is partly due to the difficulties involved in developing easy bulk crystal growth techniques for each new material and also because of historical reasons. Two materials for which thorough research and bulk crystal growth and polishing methods have already been developed are GaAs and InP.

There are three main modes of epitaxial growth: (a) monolayer, (b) nucleated and (c) nucleation followed by monolayer. Monolayer growth occurs when the deposited atoms are more strongly bound to the substrate than they are to each other. The atoms aggregate to form monolayer islands of deposit which enlarge and eventually a complete monolayer coverage has taken place. The process is repeated for subsequent layer growth. In case of nucleated growth, the initial deposit atoms

aggregate as small three-dimensional (3D) islands which increase in size as further deposition continues until they touch and intergrow to form a continuous film. This mode is favoured where the forces of attraction between the deposited atoms is greater than that between them and the substrate. In the final mode, growth starts with the formation of a single or few monolayers on the substrate followed by subsequent nucleation of 3D islands on top of these monolayers.

4.2.1 Epitaxial Lattice Matching

Epitaxy, although a highly successful approach for growing a wide range of materials, none the less suffers from an important constraint. Epitaxial growth requires that the atomic spacing, the lattice constant, of the layer material not differ by more than a few percent and that they have the same crystal structure. While most materials of interest have diamond structure, satisfying the latter requirement, the lattice matching imposes a serious constraint on the range of compositions that can be grown on a given bulk substrate. Although, traditionally, these were provided by GaAs and InP, increasing use is being made of InAs and GaSb as the substrate.

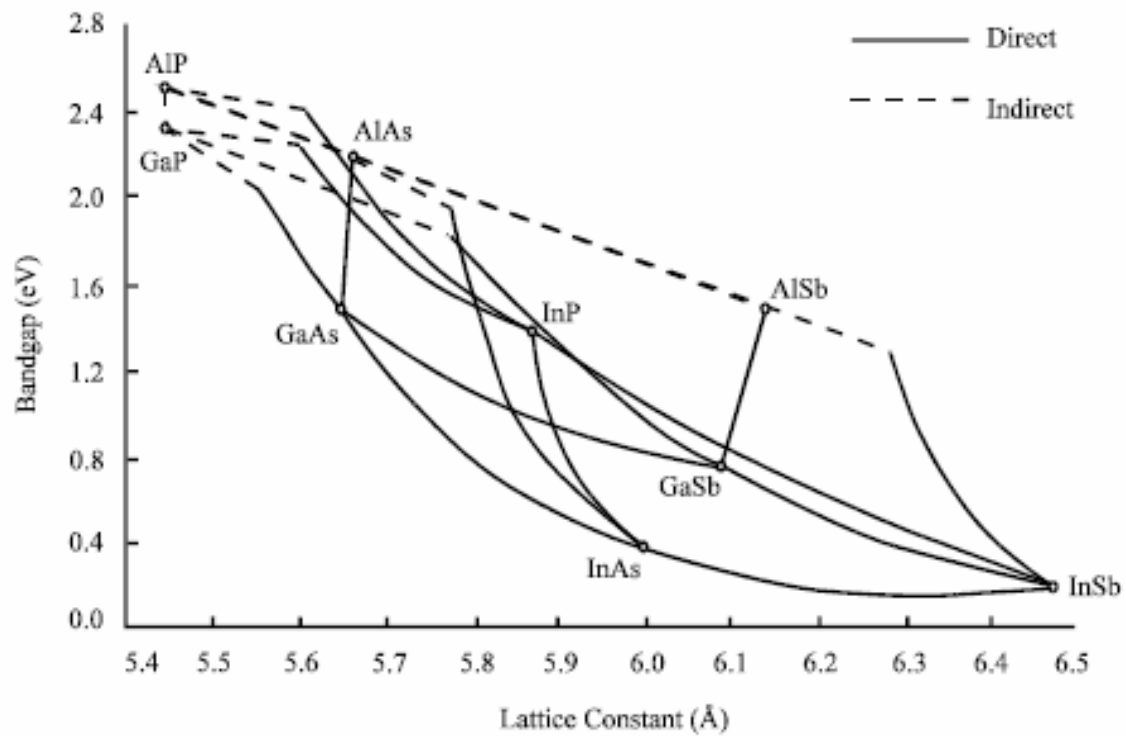


Figure 4.1: Energy bandgap and lattice constant for major III-V compounds



This problem is best appreciated by a graph of the energy gap versus lattice constant for major III-V compounds, as shown in Figure 4.1. This is also known as a phase diagram. For a possible range of ternary alloy systems, a solid line is generated between the starting binary materials. In the case of a quaternary compound, the boundary is laid out by four intersecting lines.

The ability to tailor the bandgap of III-V alloys to a desired wavelength makes them particularly attractive for optoelectronic applications. The dark currents are significantly reduced in compound detectors from their Ge and Si predecessors. In

addition, heterojunction structures can be easily used to enhance their high speed operations. One such system that is of great interest is the InP/InGaAs heterostructure which is sensitive to 1.55 μ m wavelength. In this case the composition of In_{0.53}Ga_{0.47}As ternary compound, with the desired bandgap of 0.75 eV, is dictated by the lattice matching constraint to the InP substrate.

Lattice mismatch, on the other hand, manifests itself in the form of dislocation -induced junction leakage and low quantum efficiency in optoelectronic devices.

4.3 GaN LED Process

- 1. wafer cleaning**
- 2. Mg activation**
- 3. photolithography for P -type mesa patterning**
- 4. metal mask-Ti/Al/Ni Deposition**
- 5. ICP Etching**
- 6. n-type Electrode Formation(Ti/Al/Ni/Au)**
- 7. Anneal**
- 8. Transparant Conductive Layer Deposition**
- 9. P-type Electrode Formation**
- 10. Anneal**



4.4Fabrication process of 1D-PC LED

The complete 1D PC LED process is ITO LED process and 1D PC structure coating process . Here we show the ITO LED process in detail , and the 1D PC structure coating process that include the preparation work and the optoelectronic characteristics measurement .

Step A : ITO-LED process



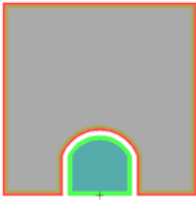


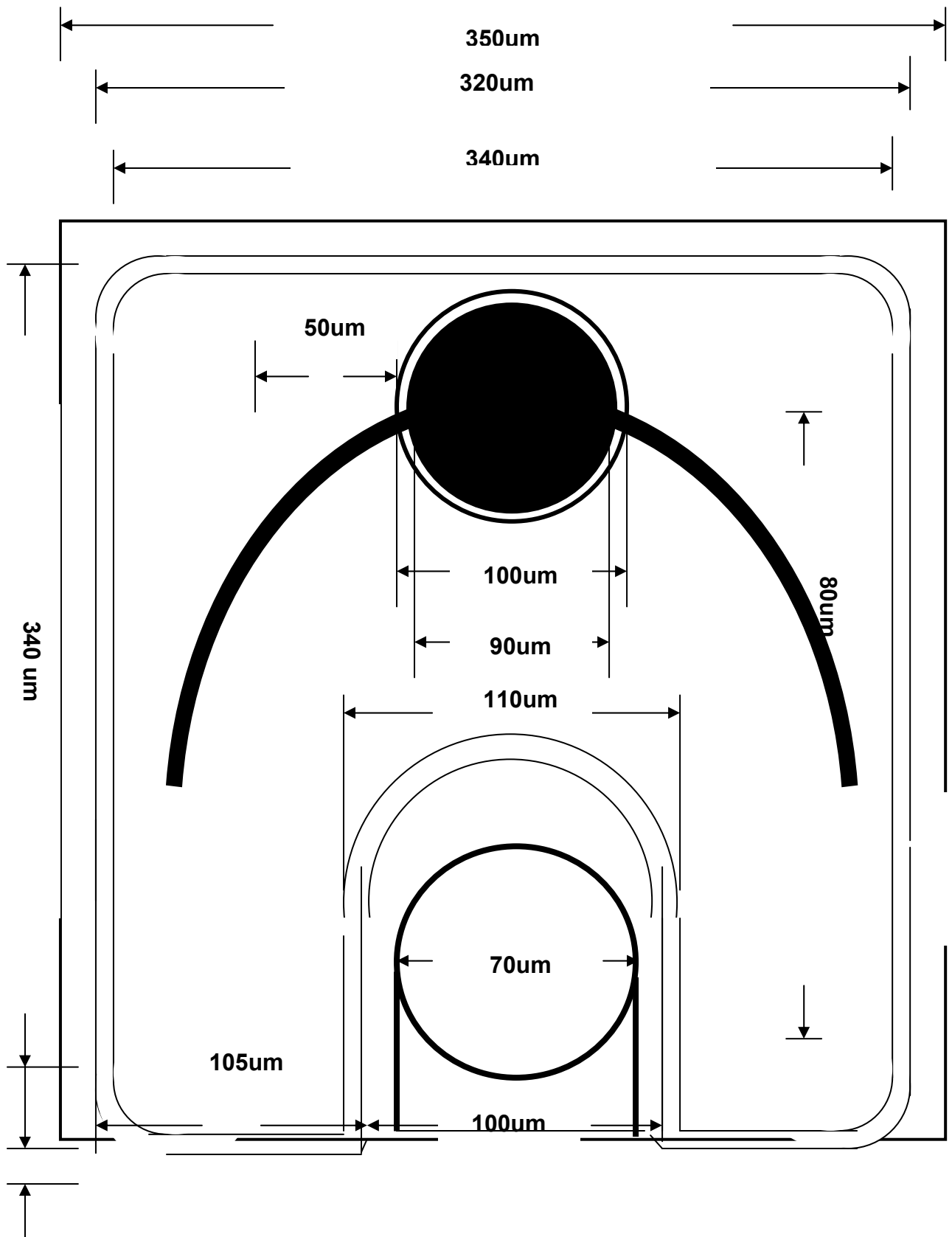
Mask NO.		Layout
Mask-1	MESA	
Mask-2	ITO	
Mask-3	ITO	
Mask-4	ELECTRODES	
Mask-5	PASSIVATION	

Table 4.1 Masks



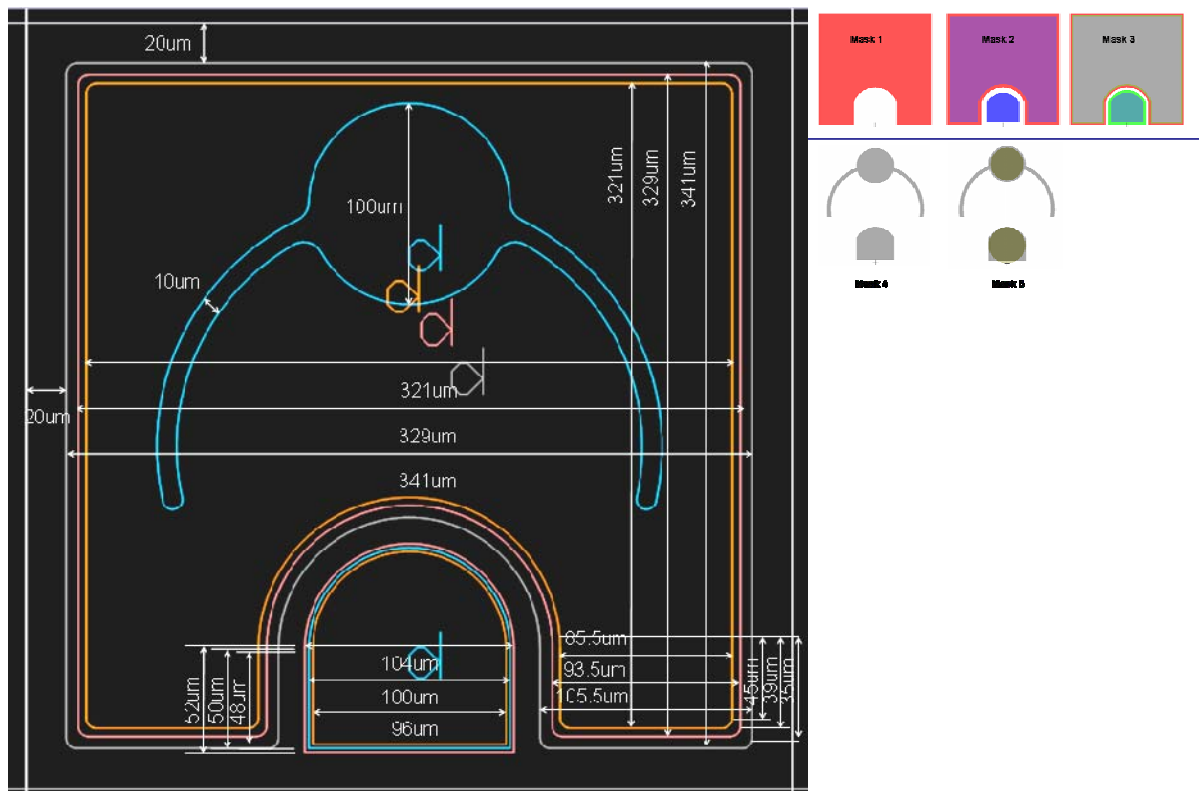


Figure 4.2 Detailed mask design

Procedures : The Processed wafers used for measure the improvement after ID

PhC structure coating :

Step01: Sapphire substrate lapping to $90 \pm 10 \mu\text{m}$

Step02: Sapphire surface polishing to mirror like surface

Step03: Wax cleaning using acetone, IPA and DI water

Step04: Electrical and optical test (chips on wafer) by wafer mapping probe before
1D-PhC structure coating

Step05: 1D-PhC structure coating by optical thin film coating machine
(OPTORUN Model 320)

Step06: Electrical and optical test (chips on wafer form) by wafer mapping probe after
1D-PhC structure coating

Step07: Wafer dicing and package in Lamp and TO CAN

Step08: Electrical and optical test of LED in package form

Table 4.2 1D PC LED Chip-process

Step	Sub-process	Mask	Condition
Clean	0.1 Surface Clean		HCl, H ₂ O, H ₂ SO ₄ = 1: 1: 3 Acid solution 30min
	0.2 Clean		DI water, 4 cycles
Mesa	1.1 Clean		Acetone; IPA; DI water, 4 cycles
	1.2 Baking		120C, 30min
	1.3 SiO ₂ growth		PECVD, 700nm
	1.4 Clean		DI water 4 cycle
	1.5 Baking		120C, 30min
	1.6 HMDS		HMDS, 15min
	1.7 PR coating		PR 204, 4K/30sec 110C, 1min baking
	1.8 Photolithography	Mask-1	8.3 sec
	1.9 Development		FHD-5, 1 min
	2.0 Baking		120C, 30min
	2.1 Discum		70C, 0.7 min
	2.2 SiO ₂ Wet etching		BOE, 4 min
	2.3 PR strip		Acetone, IPA, DI water 4 cycles
	2.4 Baking		120C, 30min
	2.5 Dry Etching		ICP, 1 min
	2.6 SiO ₂ strip		BOE, > 10min
	TEST		
ITO	3.1 Clean		Acetone; IPA; DI water, 4 cycles
	3.2 Pre-treatment		H ₂ SO ₄ : H ₂ O = 1:3 HCL: H ₂ O = 1:1 (10min, 5min)
	3.3 ITO Deposition		AST, Fuline Tech
	3.4 TEST		

P-sprd	4.1 Clean		Acetone, IPA, DI water 4 cycles
	4.2 Baking		120C, 30min
	4.3 PR coating		PR204, 4K/30sec 110C, 1min baking
	4.4 Photolithography	Mask-2	8.3 sec
	4.5 Development		FHD-5, 1min
	4.6 Baking		120C, 30min
	4.7 Discum		70C, 0.7min
	4.8 Wet Etching		HCL: HNO3 = 1:3 ;ITO (150nm/min)
	TEST		
	4.9 Clean		Acetone, IPA, DI water 4 cycles
	4.10 Baking		120C, 30min
	4.11 PR coating		PR204, 4K/30sec ,110C, 1min baking
	4.12 Photolithography	Mask-3	8.3 sec
	4.13 Development		FHD-5, 1min
	4.14 Baking		120C, 30min
	4.15 Discum		70C, 0.7min
	4.16 Wet Etching		HCL: HNO3 = 1:3 ITO (150nm/min)
	I-V TEST		
Pad	5.1 Clean		Acetone, IPA, DI water 4 cycles
	5.2 Baking		120C, 30min
	5.3 PR coating		PR5214, 4K/30sec 90C, 1.5min baking 110C, 3min post baking
	5.4 Photolithography	Mask-4	2 sec, 11sec (FL)
	5.5 Development		FHD-5, 1min
	5.6 Discum		70C, 0.7min
	5.7 E-beam Evaporation		Ni(250nm)/Au(250nm) 3A/sec: 3A/sec
	5.8 Lift Off		Acetone, IPA, DI water 4 cycles
	I-V TEST		

Passivation	6.1 Clean		Acetone; IPA; DI water, 4 cycles
	6.2 Baking		120C, 30min
	6.3 SiO ₂ growth		PECVD, 700nm
	6.4 Clean		DI water 4 cycle
	6.5 Baking		120C, 30min
	6.6 HMDS		HMDS, 15min
	6.7 PR coating		PR204, 4K/30sec
	6.8 Photolithography	Mask-5	8.3 sec
	6.9 Development		FHD-5, 1min
	6.10 Baking		120C, 30min
	6.11 Discum		70C, 0.7min
	6.12 Wet etching		BOE, 4min
	6.13 Clean		DI water 4 cycles
PhC Structure	7.1 Clean		Acetone; IPA; DI water, 4 cycles
	7.2 Pre-treatment		H ₂ SO ₄ : H ₂ O = 1:3 HCL: H ₂ O = 1:1 (10min, 5min)
	7.3 ITO Deposition		AST, Fuline Tech
	7.4 TEST		

4.5 Simulation of PhC Structure

Optimization of the 1D-PhC structure for Blue LED by theoretical modeling

Software: *Essential Macleod*

PhC ODR Structure- α

Layer No	Material	Thickness (nm)
1	TiO ₂ (n=2.5)	53.33
2	SiO ₂ (n=1.42)	211.89
3	TiO ₂	56.16
4	SiO ₂	104.22
5	TiO ₂	44.47
6	SiO ₂	100.31
7	TiO ₂	52.1
8	SiO ₂	99.53
9	TiO ₂	49.18
10	SiO ₂	115.55
11	TiO ₂	61.31
12	SiO ₂	54.9
13	TiO ₂	0
14	SiO ₂	109.62
15	TiO ₂	33.95

TiO₂ (n=2.5) , SiO₂(n=1.42) @

Table 4.3 Simulation: 1D-PhC structure of blue LED:

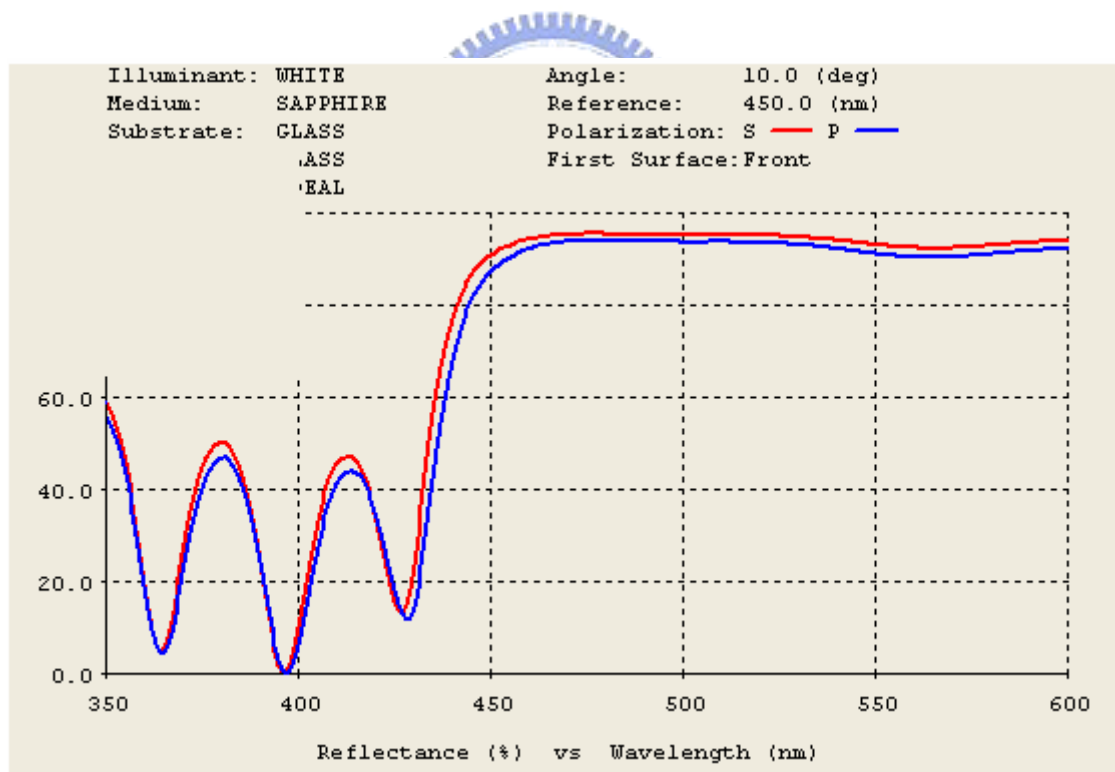
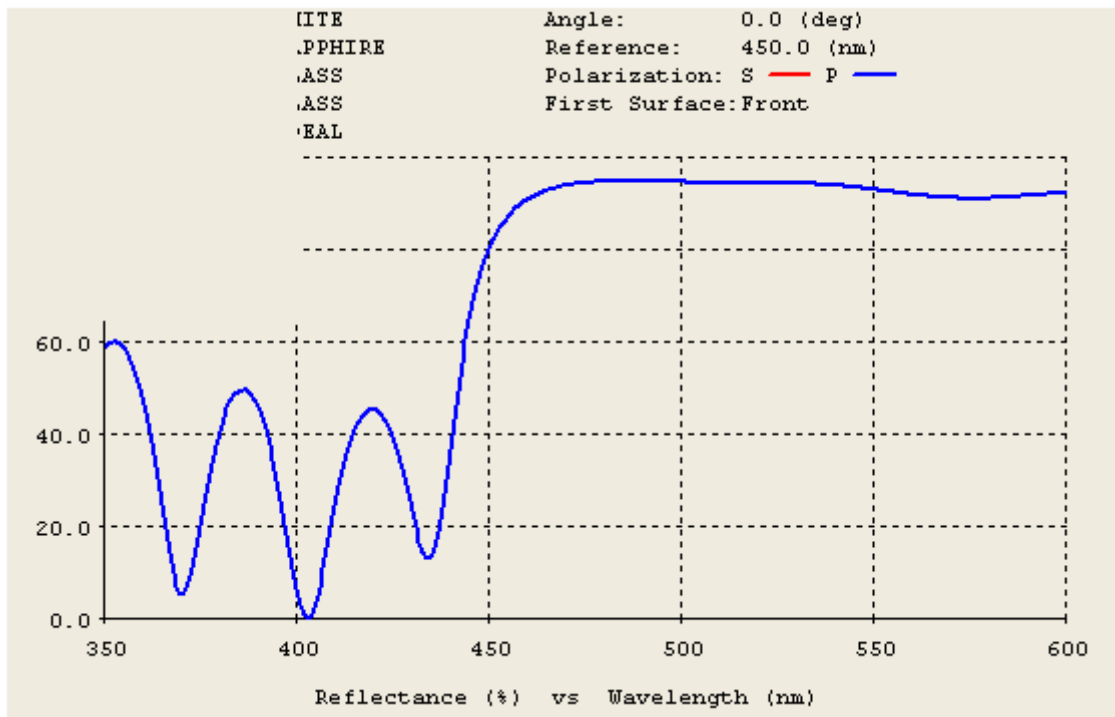
Optimization of the 1D-PhC structure for Blue LED by theoretical modeling

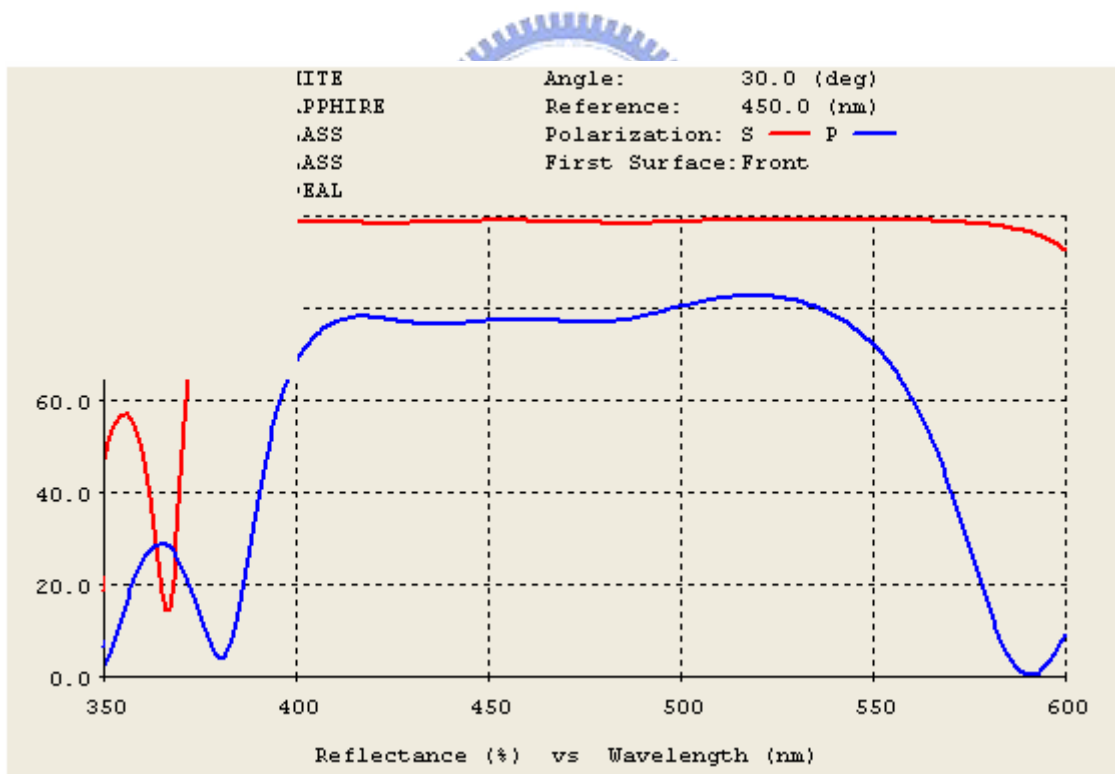
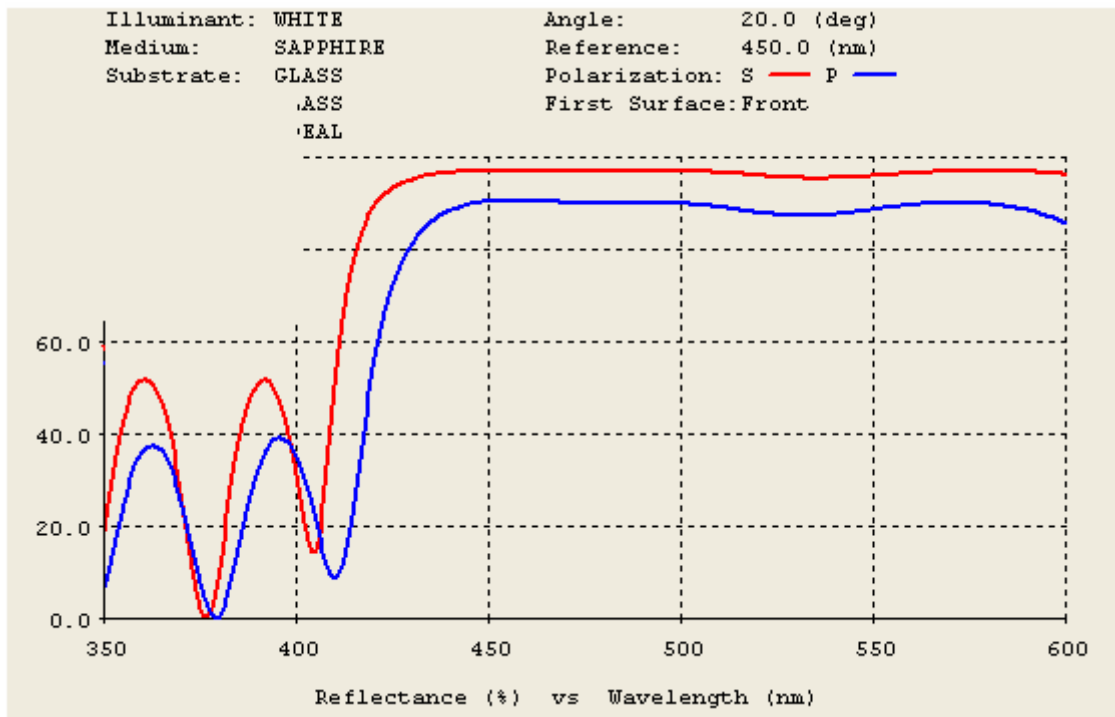
Software: *Essential Macleod*

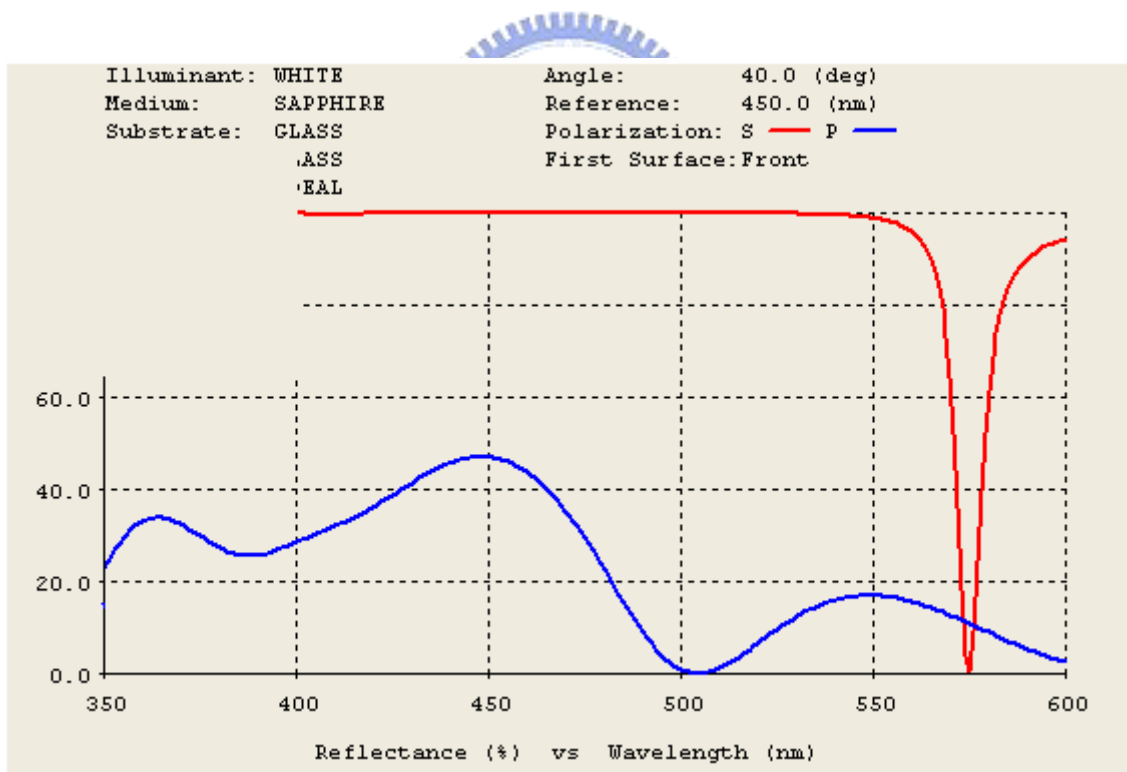
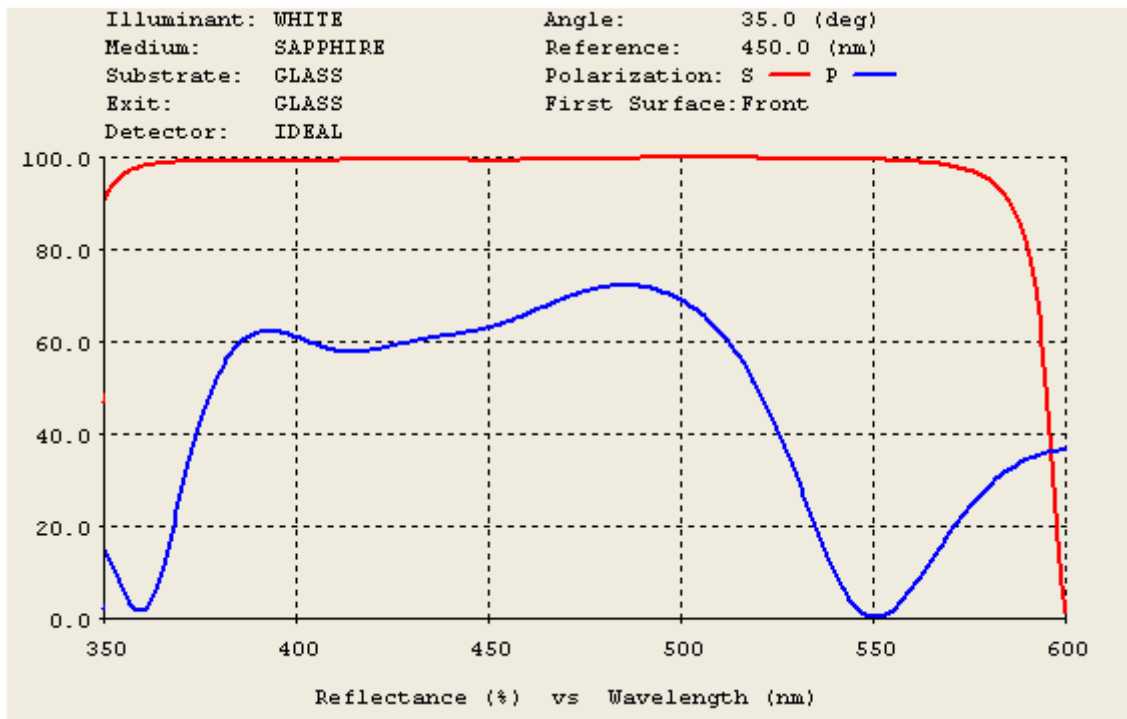
PhC ODR Structure-β

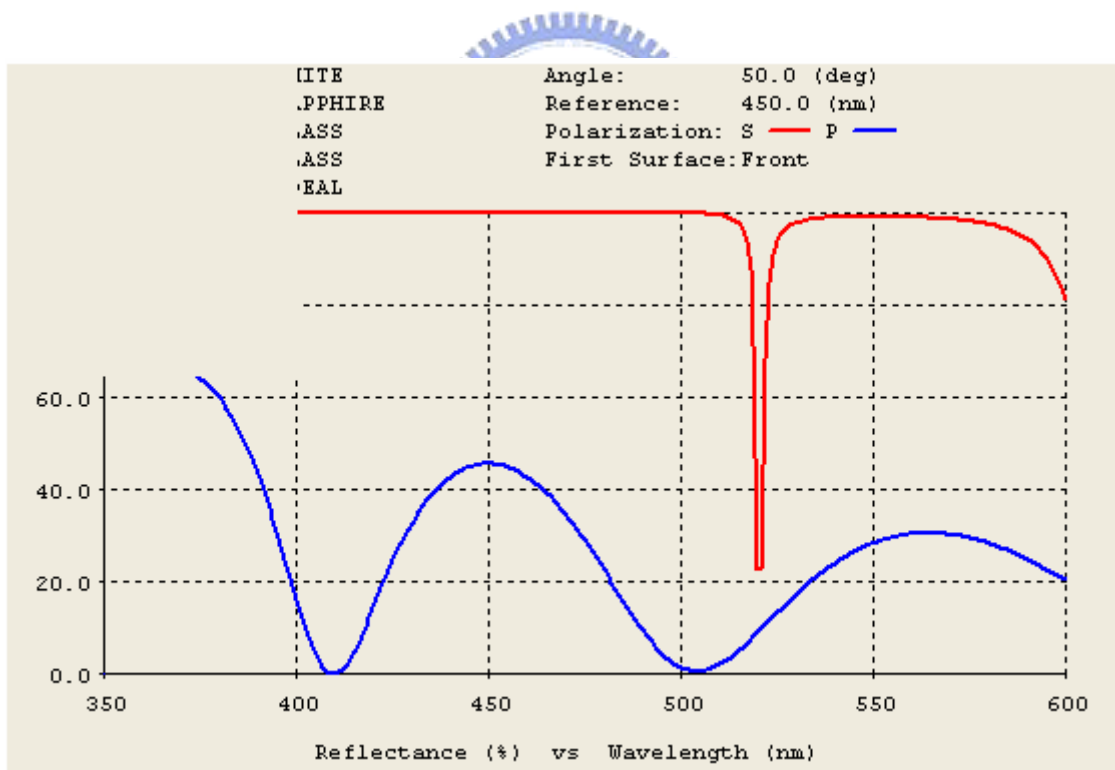
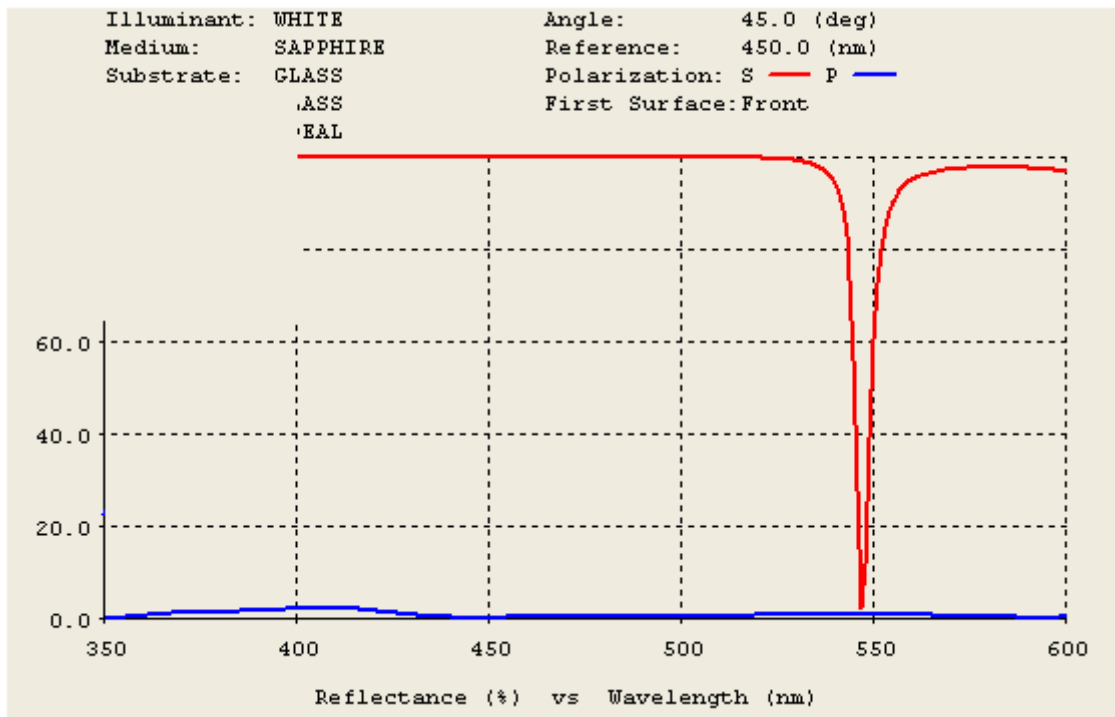
Layer No	Material	Thickness (nm)
1	Ta ₂ O ₅ (n=2.1~2.23)	67.43
2	SiO ₂ (n=1.42)	169.92
3	Ta ₂ O ₅	75.69
4	SiO ₂	90.09
5	Ta ₂ O ₅	64.59
6	SiO ₂	83.65
7	Ta ₂ O ₅	67.81
8	SiO ₂	83.56
9	Ta ₂ O ₅	65.96
10	SiO ₂	86.03
11	Ta ₂ O ₅	66.47
12	SiO ₂	84.56
13	Ta ₂ O ₅	26.89
14	SiO ₂	121.52
15	Ta ₂ O ₅	60.48

Table 4.4.Simulation: 1D-PhC structure of LED









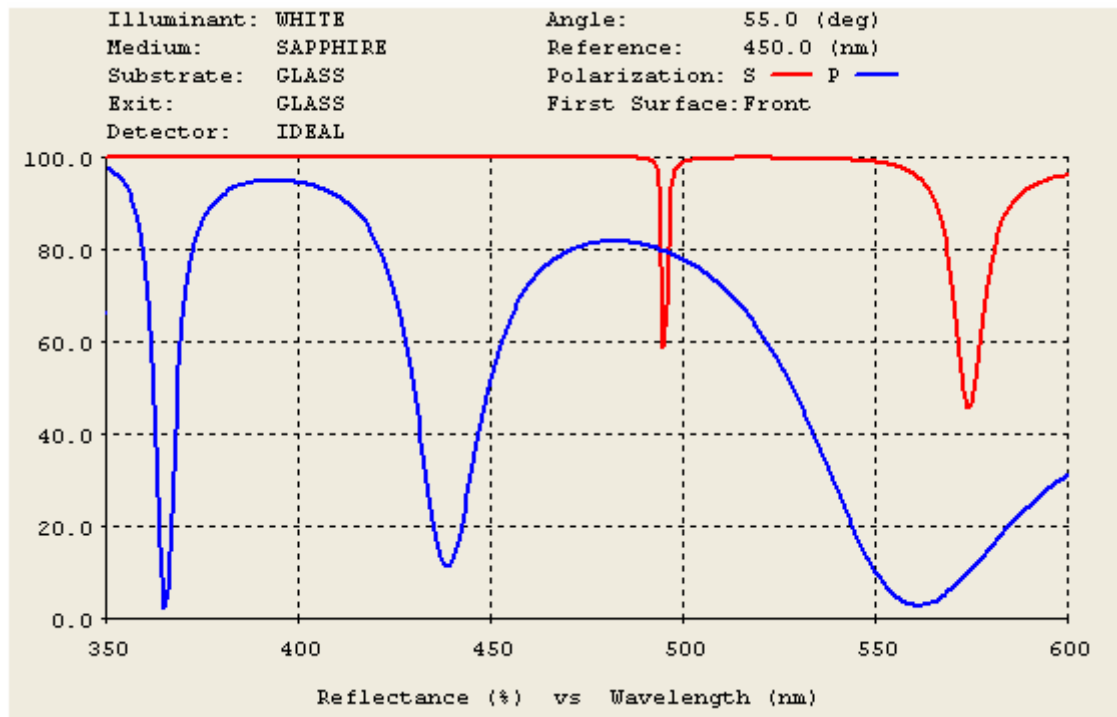


Figure.4.3 .Simulation: reflection spectrum for blue LED



Chapter 5.

Experimental Results and Discussion

In this chapter , we show the experimental results (measurement data) of

1. Light emission mapping result before and after dielectric layers of photonic crystal structure coating on the sapphire-face (backside) : Then we see the big improvement in light output that almost doubles the LOP of the processed half-cut wafer before PC-ODR layers coating .
2. Axial emission measurement in lamp-form : Here we choose the lamp-package of narrower view angle , then we can see the strong emission enhancement at axial direction clearly if the LED chips have PC-ODR films.
3. Measurement of NiAu ,ITO and PC LEDs in lamp-form : Comparing the light output of ITO LED to NiAu LED , we can see the bigger light extraction of ITO LED due to the higher ITO transparency . Comparing PC LED to ITO LED in lamp form (lamp package has the silver paste and the die-cup to be the reflector) , PC LED has the higher photometric intensity (lm , $lm/watt$) due to the red-shift ,even though their radiometric intensity is very closed .
4. Radiation pattern measurement of NiAu , ITO and PC LEDs packaged in TO can : We put the bare LED chip on TO-can without any material coating on this chip in order to obtain the information of the emission intensity distribution in all emitting

angle. We find the very big jump in light extraction ability between NiAu and ITO LED ; between ITO and PC LED ,respectively .

5.1. Light Emission Mapping Result of Half-cut wafer


The purpose of this light emission mapping is to find the increasing percentage after LED chips added Photonic Crystal reflector , and show the results of different photonic crystal structure of two kinds of material composition , PhC-structure- α : $\text{TiO}_2/\text{SiO}_2$ and PhC-structure- β : $\text{Ta}_2\text{O}_5/\text{SiO}_2$. Both of the two PhC structures are 7 pairs + 1 layer .(15 layers) .

❖ 01 - Samples : #01-301C, #02-301A, #03-301D, #4-2822A .

(InGaN-based LED before and after photonic crystal ODR layers coating)

❖ 02 - Test equipment : LED mapper MP - WeiMin ,model LED 628

❖ 03 - Test result :



Sample	#01 - 301C	#02 - 301A	#03 - 301D	#04 - 2822A
PhC-structure	PhC-structure- α	PhC-structure- β		
Emission Improvement	104%	95%	110%	96.5%
Sample Amount	3219	2415	3829	3164

Measurement condition : $I_F = 20\text{mA}$

PhC-structure- α and PhC-structure- β are the designed structures mentioned in section 4-5 .

Table 5-1 Light emission mapping result of half-cut sample wafers before and after PC-ODR layers coating

◆ Axial Power Improvement calculation using mapped data .,

$$110 \% = \frac{[\sum_{j=1 \text{ to } 3829} (L_{\text{ODR-j}} \times \#_{\text{ODR-j}})] - [\sum_{k=1 \text{ to } 3829} (L_{\text{No ODR-k}} \times \#_{\text{No ODR-k}})]}{[\sum_{k=1 \text{ to } 3829} (L_{\text{No ODR-k}} \times \#_{\text{No ODR-k}})]}$$

◆ Concluding remarks :

- 1./ Using the two PhC ODR- structures, α , β , the LOP is doubled compared to the sample before PC layers coated .

- 2. /. The causes of the spreading of LOP (before & after PC-film Coating) are :

2.a./ The LOP increasing factor should be constant , η , at a fixed angle .

The sample before PC-layers coated , the LOP spreading is $\Delta \text{LOP}_{\text{bf.PhC-ODR}}$.

Then after coating PC- layers , the LOP range should be spreading to a bigger range $\eta \times \Delta \text{LOP}_{\text{bf.PhC-ODR}}$.(where $\eta > 1$) .

2.b./ A little bit non-uniformity of the PC-layers also resulted in spreading of LOP.

(See the measurement data below)

❖ 04 -Light Output Maps and Statistics of 4 samples with and without PC-layers:

#01 - 301C / PhC-structure -α

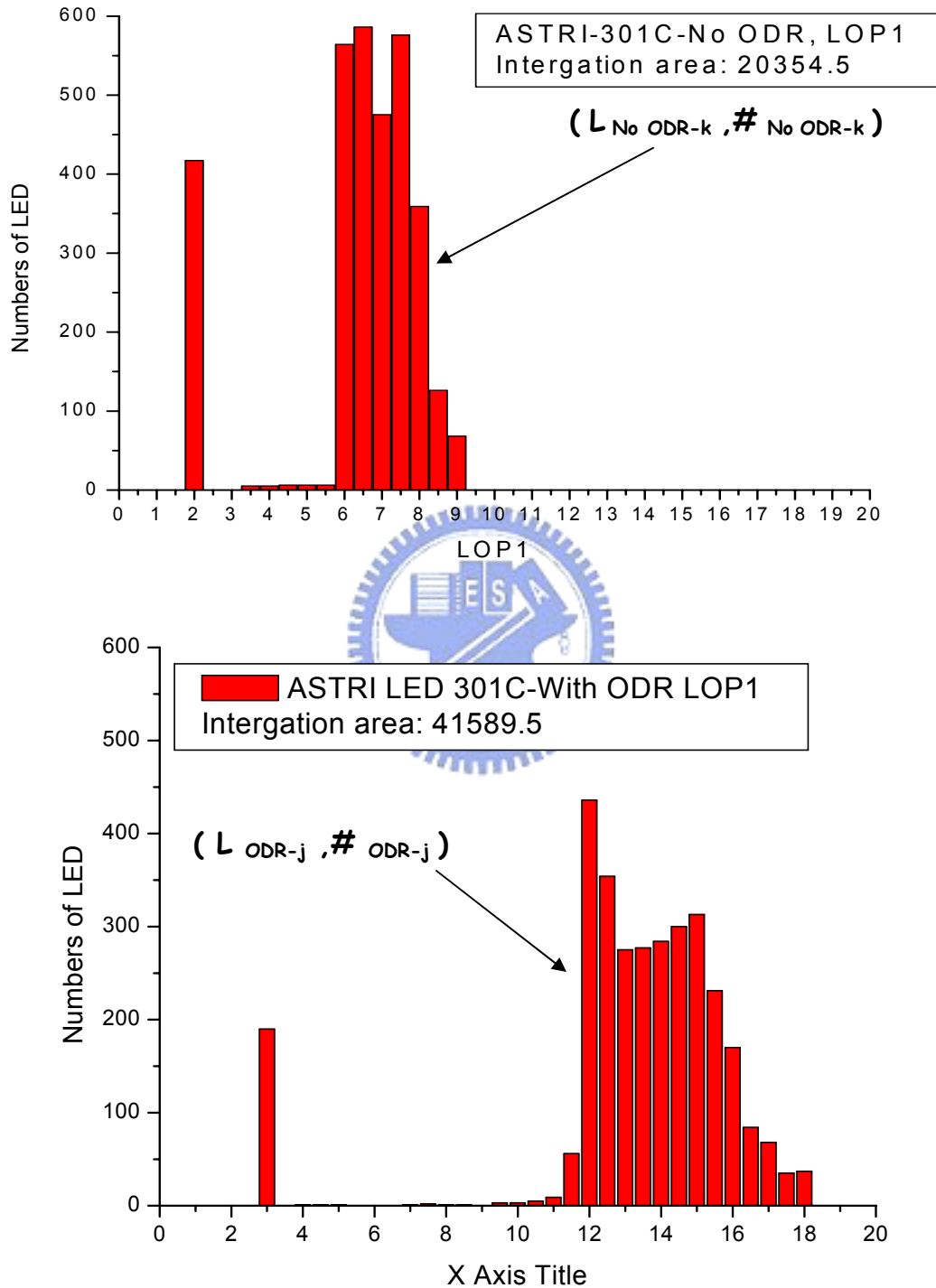
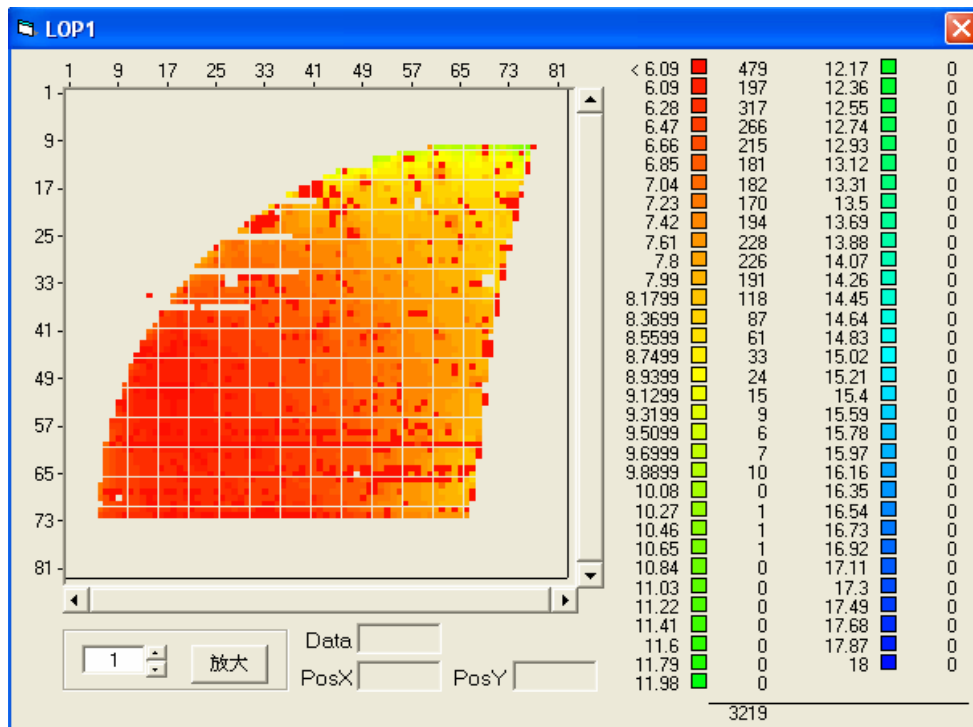
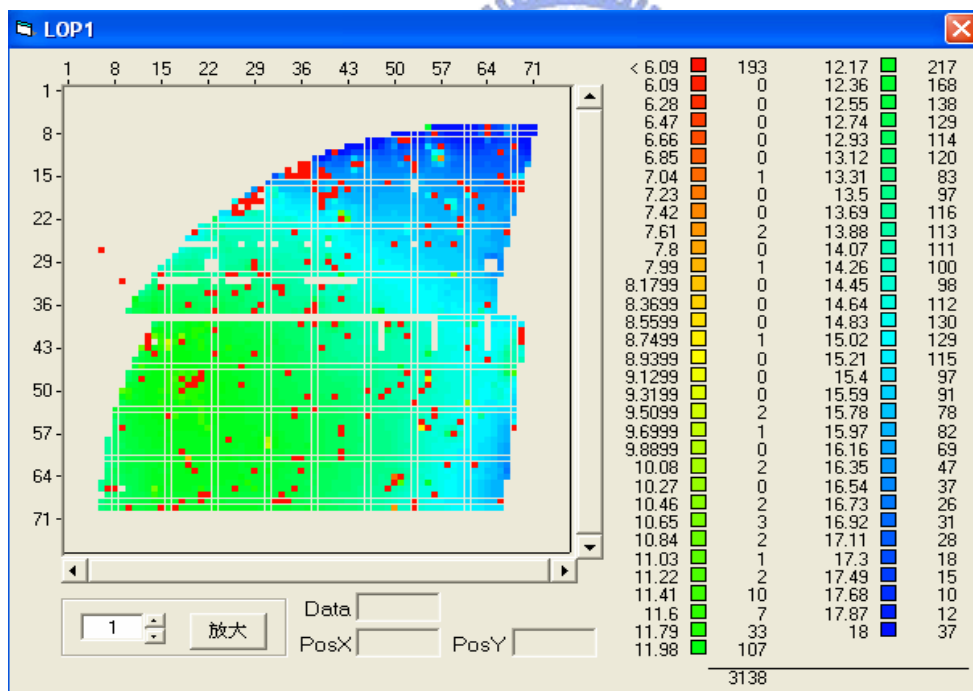


Fig.5-1 LOP Distribution of #01-301C with and without PC ODR Structure



301 C – No PhC-structure



301C –PhC-structure

Fig.5-2 Raw data of LOP Distribution of #01-301C with and without PC ODR structure

#02 - 301A / PhC-structure - β

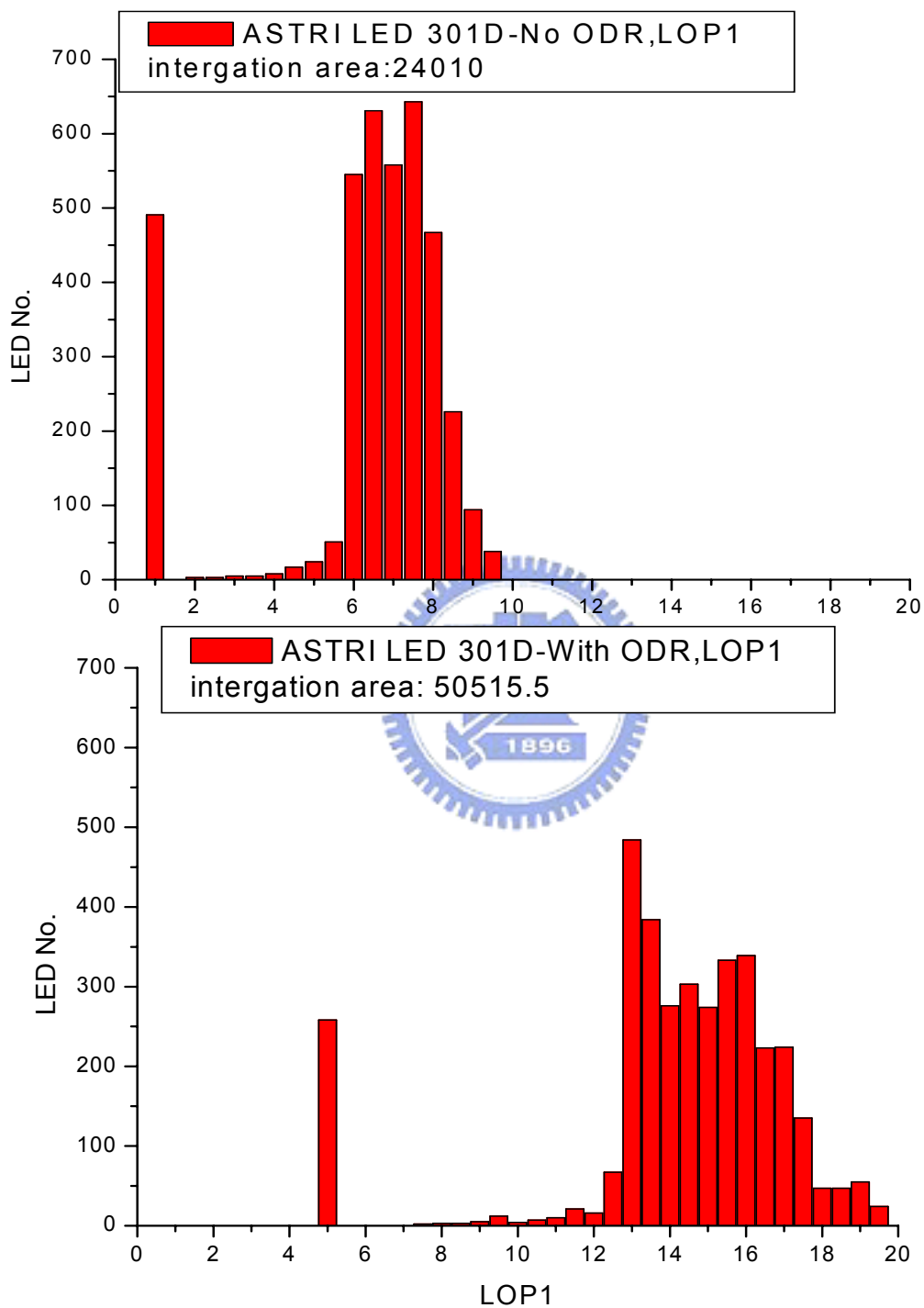


Fig.5-3 LOP Distribution of #02-301A with and without PC ODR structure

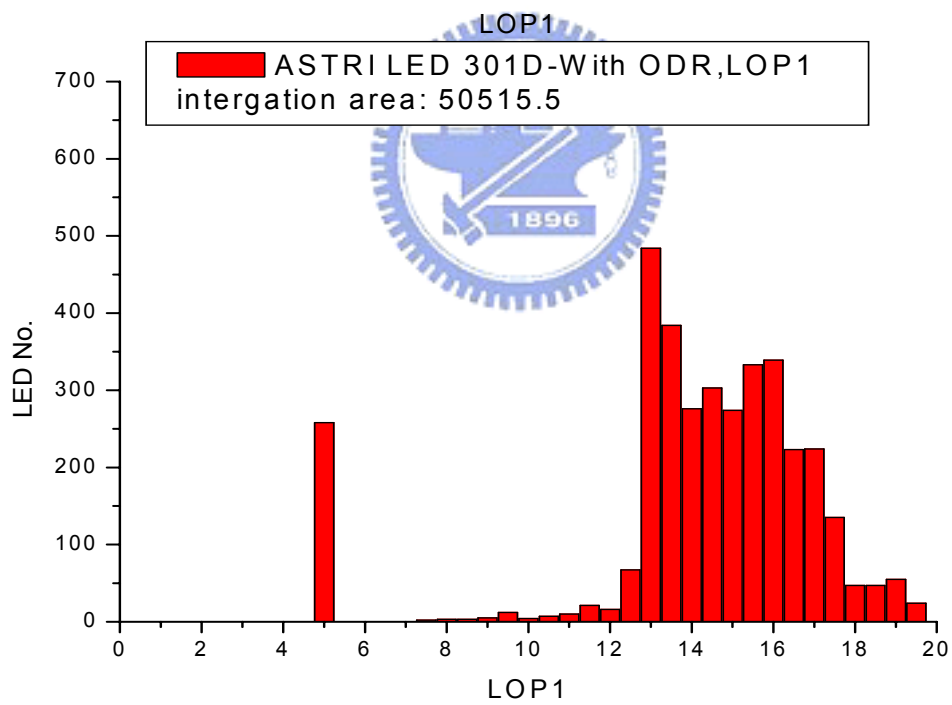
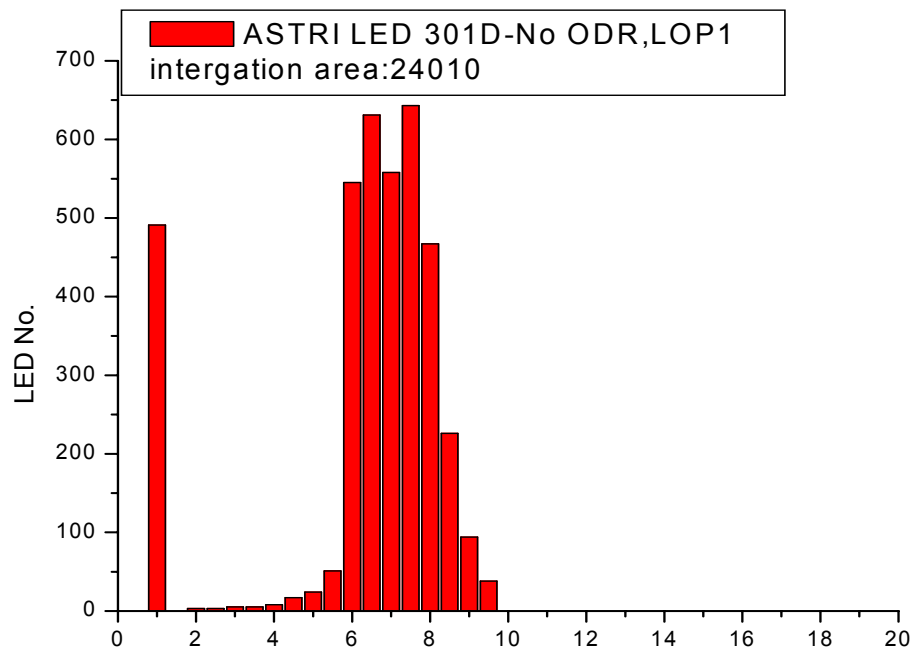
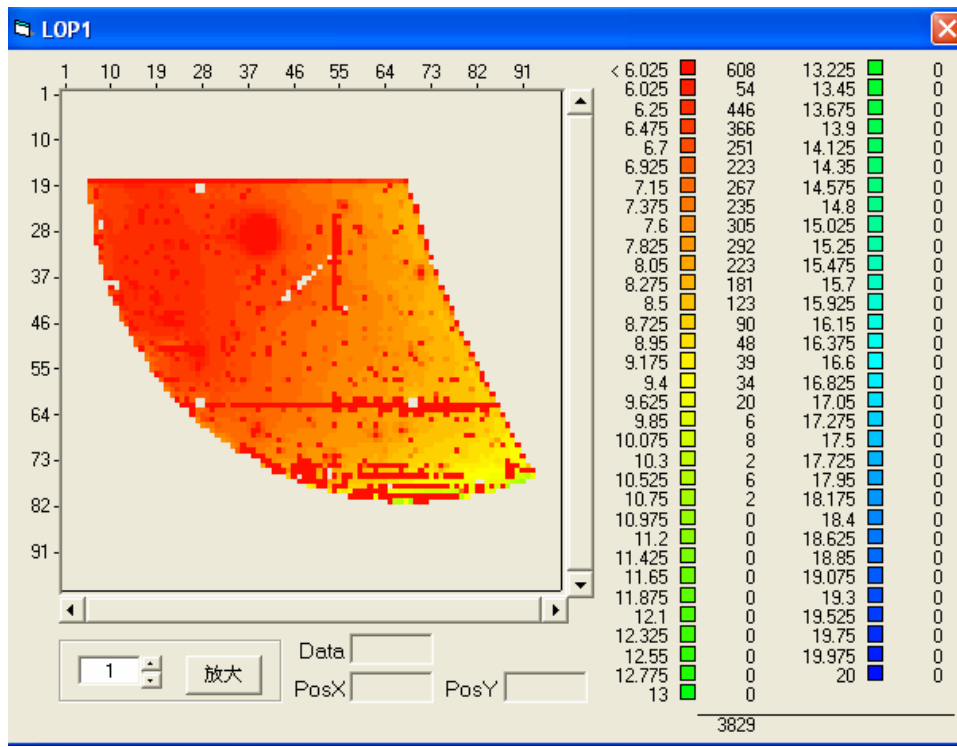
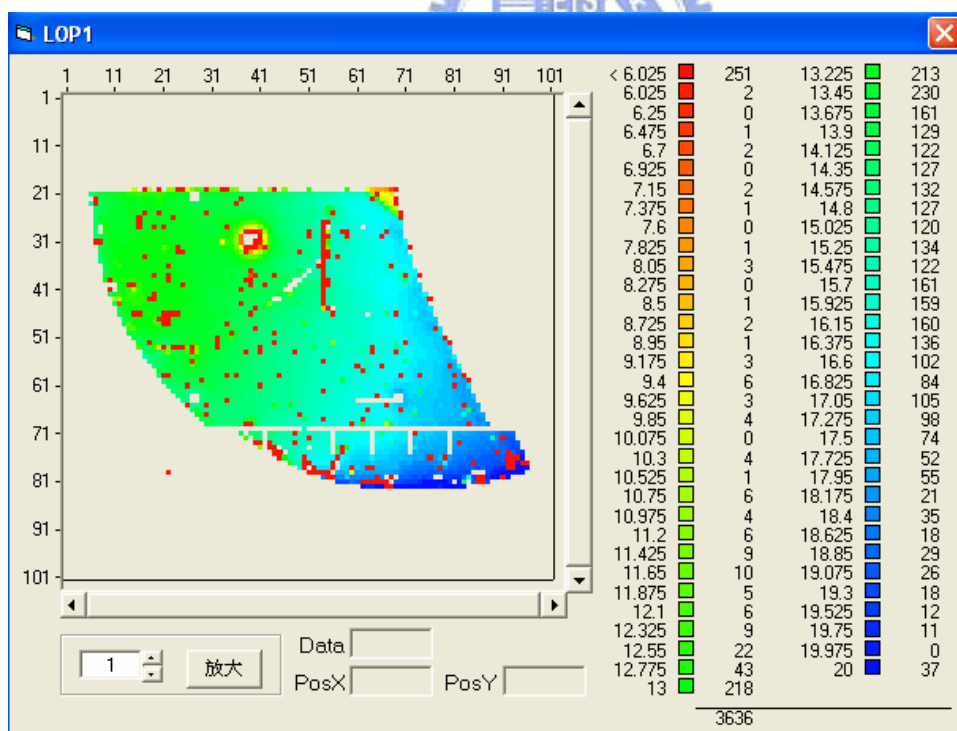


Fig.5-5 LOP Distribution of #03-301D with and without PC ODR layers



301D – No PhC-structure



301D – PhC-structure

Fig.5-6 Raw data of LOP Distribution of #03-301D with and without PC ODR structure

#04 - 2882A / PhC-structure -β

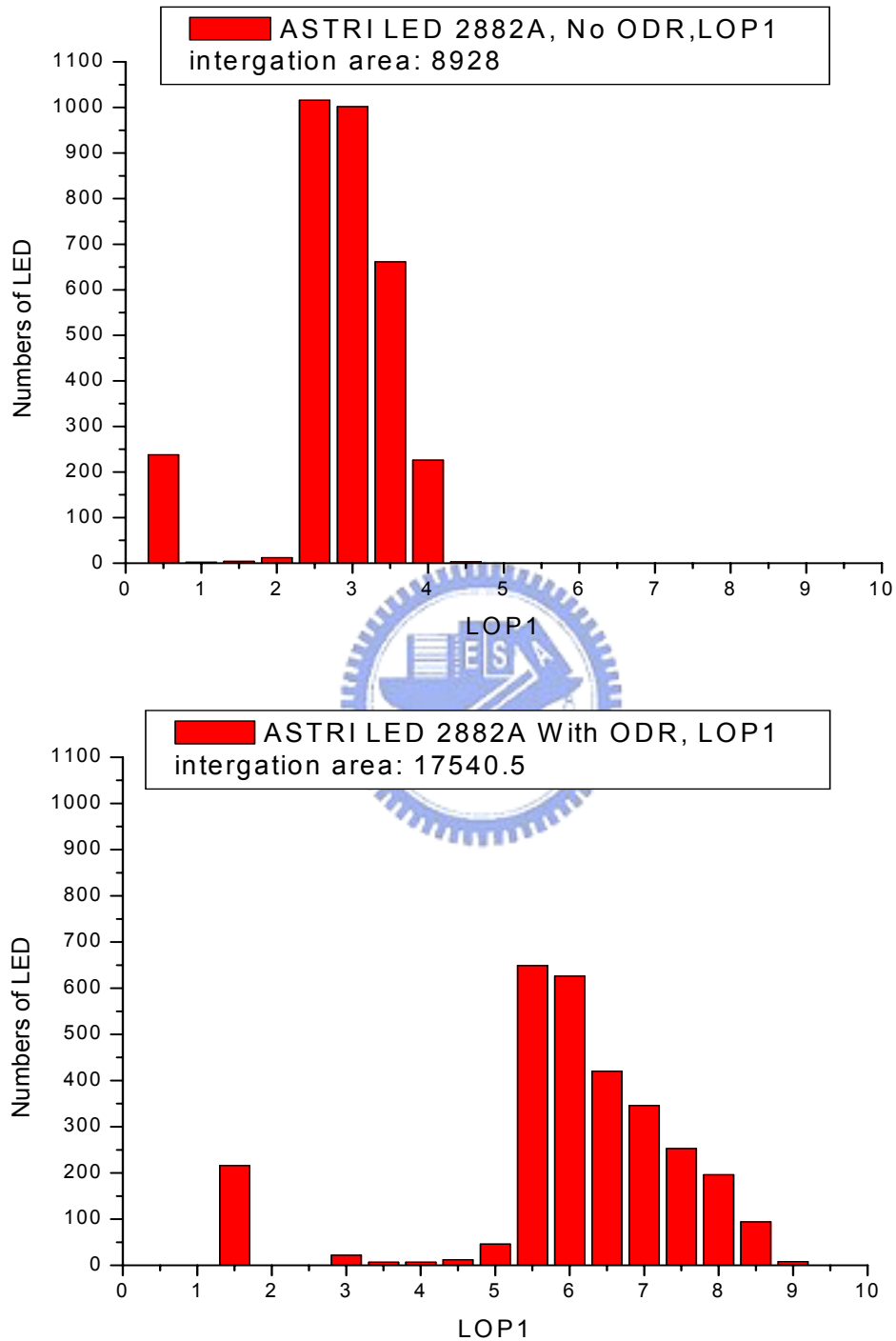


Fig.5-7 LOP Distribution of #04-2882A with and without PC ODR structure

5.2. Axial Emission Measurement in Lamp-form

Comparing the axial emission intensity of PC LED to the ITO LED, under 1. / same lamp-package , 2./ these 10 x2 LED chips are produced from the same epitaxial wafer, the average of PC LED axial I_v increases by 92.1%.

Why are we interested in the emission enhancement at axial direction ? The reasons are : The reflection loss of dielectric material (PC layers) should be lower than metal reflector . It is because the reflection mechanism of dielectric material is the dipole vibration, it will not loss energy ; on the other hand, the incident light has to share some part of energy to the mobile charge near to the surface when the light reflection happens at the metal reflector . Besides., the 1D PC reflector can also be applied to the AlInGaP LEDs by Thin –film LED technology . The epitaxial layer thickness of AlInGaP LED is around 10 μm , and the 1D PC reflector is located between the epitaxial layers and substrate of Thin-Film LED .That is, 1D PC reflector is positioned at the depth of around 10 μm . It is very shallow reflector . The axial light emission enhancement is very strong and is very useful to the narrow view angle LED device .

		AVG	#01	#02	#03	#04	#05	#06	#07	#08	#09	#10
PC LED Lamp	I _V (mcd)	390.66	463.8	451.3	363.2	445.2	335.1	382.8	442.9	354	314.5	353.5
	V _F (volt)	3.136	3.1	3.12	3.14	3.16	3.14	3.1	3.09	3.15	3.22	3.14
ITO LED Lamp	I _V (mcd)	203.39	238.2	174.1	161.7	231	234.9	206.4	158.5	230	168.7	230.4
	V _F (volt)	3.189	3.16	3.19	3.19	3.18	3.17	3.22	3.18	3.23	3.19	3.18
Axial I _v Increase %		92.1%	LED Lamp $\theta_{1/2}=15^\circ$, @ I _F = 20 mA									

Test equipment: 遠方LED620

- 1.) LED chips of these PC LED and ITO LED lamps come from the same epitaxial wafer
- 2.) The PC LED is ITO LED with 1D Photonic Crystal reflector at sapphire face(backside) .

Table 5-2 Axial emission intensity measurement of PC LED Lamps and ITO LED Lamps .

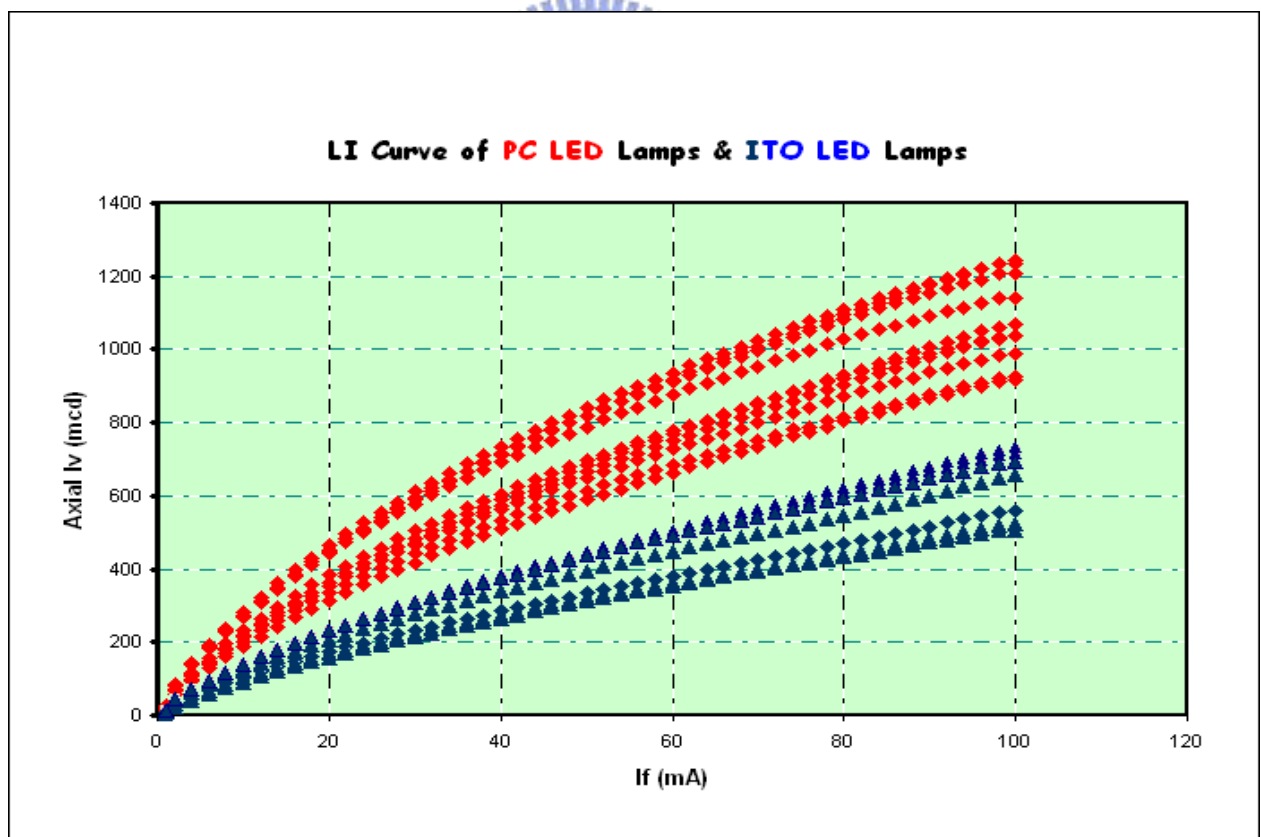


Fig.5-9 LI Curve of PC LED Lamps and ITO LED Lamps

According to the results above, the processed wafer after PC-films coating will have around 90 % axial Iv improvement . We know the major cost of LED chips is the epitaxial wafer . So, we can process the epitaxial wafers of regular grade with axial emission layer of photonic crystal structure, And obtain the higher light output especially from the lamp of narrower view angle ,

5.3. Radiometric and photometric Measurement of NiAu ,ITO and PC LED in Lamp-form

LED chips of these NiAu LED lamps,ITO LED lamps and PC LED lamps , 3 x3ea, are produced from the same epitaxial wafer. According the optoelectronic characteristics measurement results shown below, we find :

a.) Radiation power (radiometric ,mW, and photometric ,lm)of ITO LED and PC LED are much higher than NiAu LED . The TCL(Transparent Conductive Layer) of NIAu LED is NiAu layer ; The TCL of ITO LED and PC LED is ITO layer. The transparency of ITO layer (~90%) is higher than NiAu layer(~60%). So the result of NiAu LED`s lower radiation extraction is reasonable .

b.) The radiometric power of ITO LED and PC LED are very close, 11.8 mW and 11.63 mW, respectively . However, the photometric power of PC LED , 526.3 mlm, is higher than ITO LED, 468.7mlm. According to this measurement

table , we find the possible explanation ,that is , after PC-films Coating, due to the red-shift effect ($\sim 3\text{nm}$) , the emission flux (photometric) will improve 12.3% ,

HighLink sample wafer (HL 146566)

lamp $\theta_{1/2}=7.5^\circ$

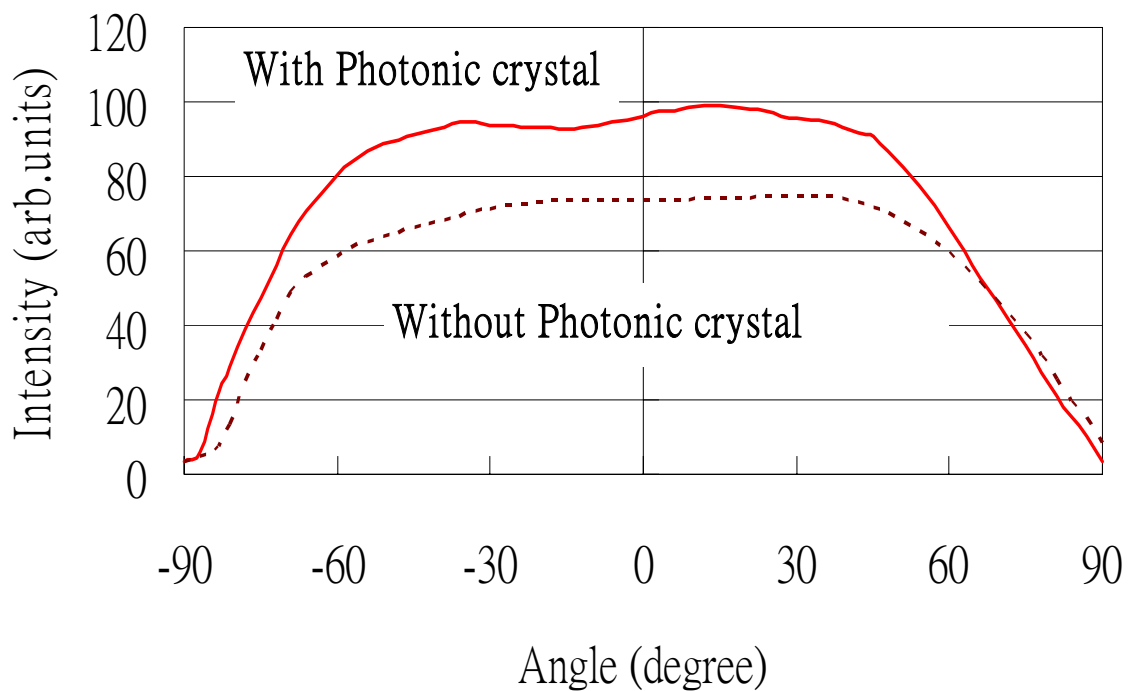
@20mA		Vf	mW	mlm	$\lambda_P(\text{nm})$	$\lambda_D(\text{nm})$	WH(nm)	lm/W
Ni/Au LED	1	3.21	6.9	237	448	455	21	3.69
	2	3.19	6.2	226	449	455	21	3.54
	3	3.20	7.0	252	449	455	20	3.94
		3.20	6.73	238.3	448.5	455.0	20.6	3.723
ITO LED	1	3.19	11.6	474	452	458	22	7.43
	2	3.21	12.2	461	451	456	22	7.18
	3	3.20	11.6	471	452	458	22	7.36
		3.20	11.80	468.7	451.5	457.3	22.0	7.323
PC (+ITO) LED	1	3.18	12.3	480	451	457	20	7.55
	2	3.15	11.0	571	458	463	23	9.06
	3	3.16	11.6	528	455	460	22	8.35
		3.16	11.63	526.3	454.7	460.1	21.6	8.320

Table 5-3 Radiometric and photometric measurement of NiAu LED lamps, ITO

LED lamps and PC LED lamps.

5.4. Radiation Pattern of NiAu ,ITO and PC LEDs packaged in TO Can

In order to have the real emission pattern of LED dice , TO-can is a very useful tool . We put the bare LED die on TO-can without any material coating on this die. In this way , the measured radiation pattern will not be disturbed . Then we can obtain the information of the emission intensity distribution in all emitting angle. We find the very big jump in light extraction ability between NiAu and ITO LED ; between ITO and PC LED ,respectively .



**Fig.5-10.Radiation pattern of Blue LED with and without photonic crystal layers
(packaged in TO46)**

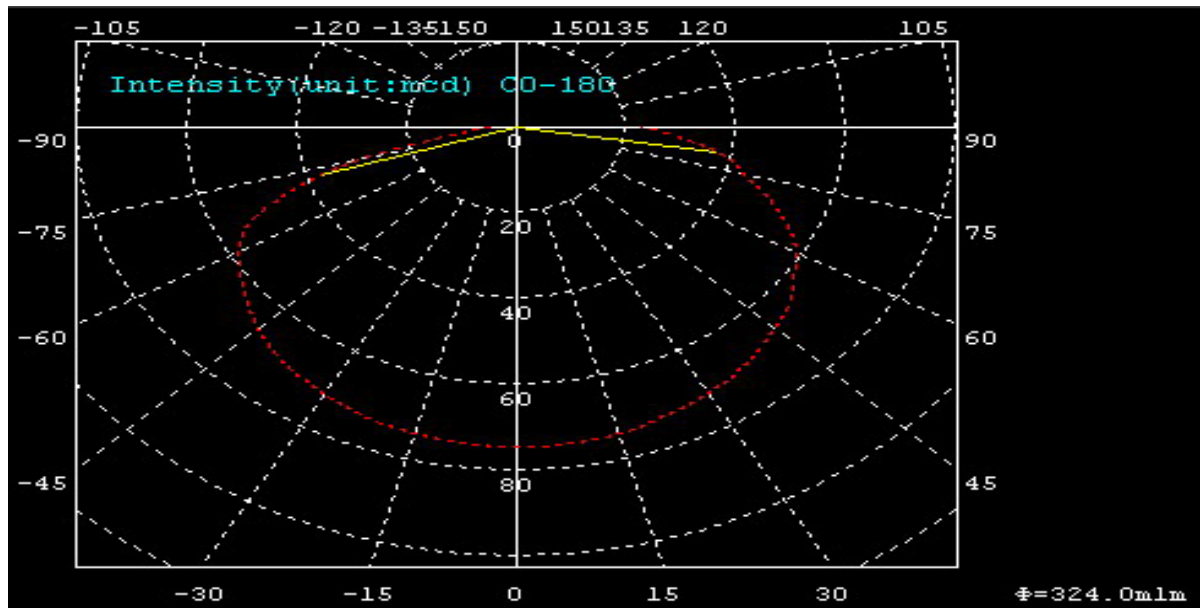


Fig.5-11. Raw data of radiation pattern of blue LED without photonic crystal

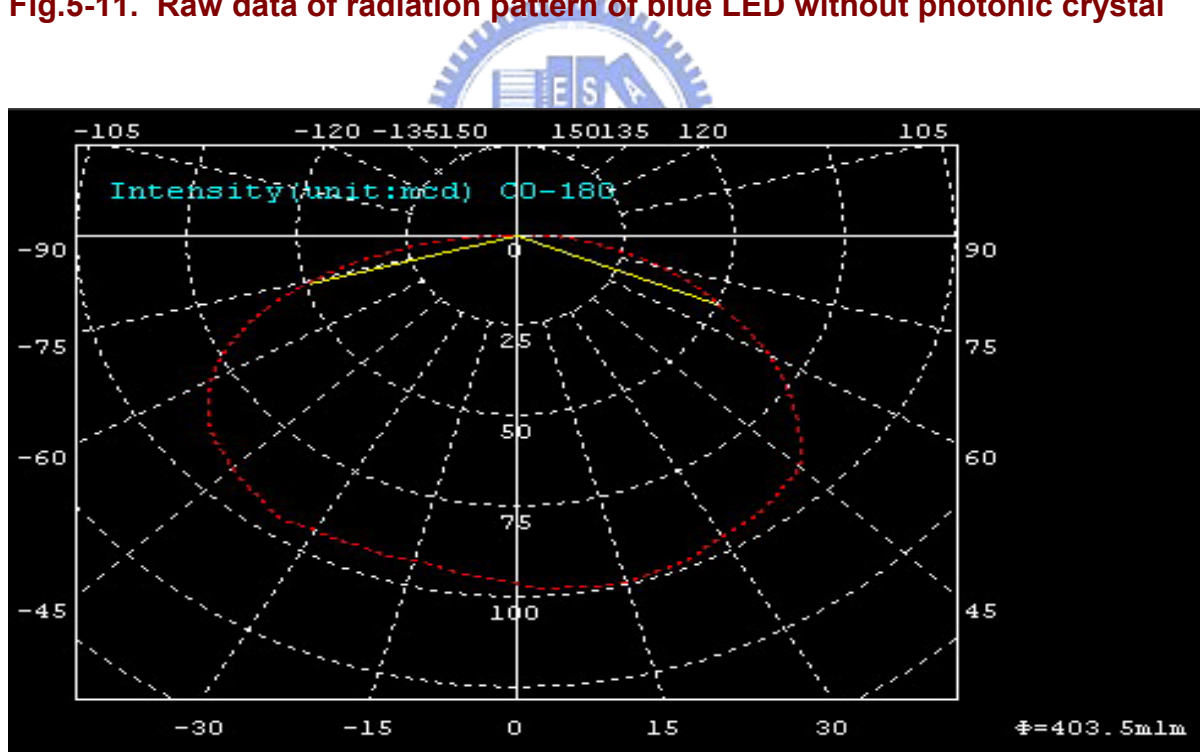
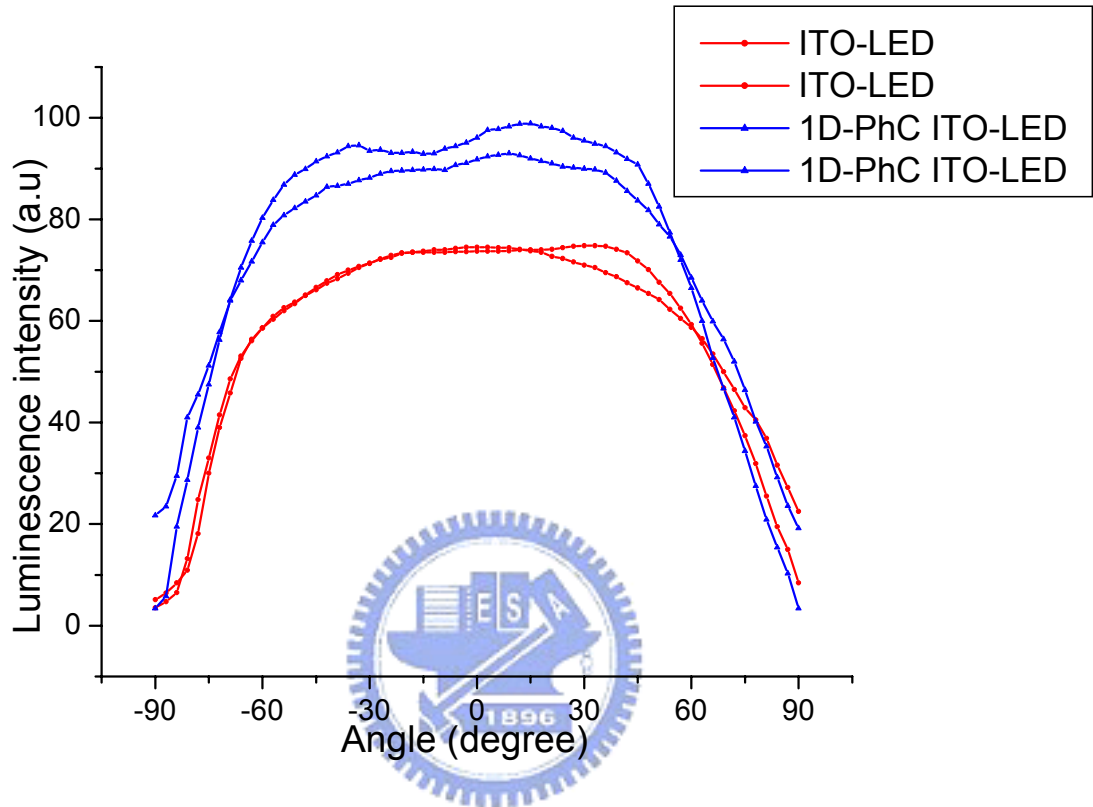


Fig.5-12. Raw data of radiation pattern of blue LED with photonic crystal

In order to make sure the result of Fig.5-10 , we measured other 2 x 2 LED dice packaged in TO46-can . All these dice are processed from the same epitaxial wafer .

And the result below shows the repeatability of the strong light extraction enhancement of PC LED.



**Fig.5-13. Radiation pattern of LED with and without photonic crystal
(PC LED and ITO LED packaged in TO46 -can)**

According to the measurement results shown above , we find the big luminous intensity at almost all emission angle can be achieved from PC LED than that of ITO LED. The PC LED has photonic crystal reflector to enhance the light extraction efficiency is the very reasonable explanation .

Following the content of the ``section 5.3. Radiometric and Photometric Measurement of NiAu ,ITO and PC LEDs in Lamp-form`` , we are interested in the radiation pattern difference between ITO LED and NiAu LED .

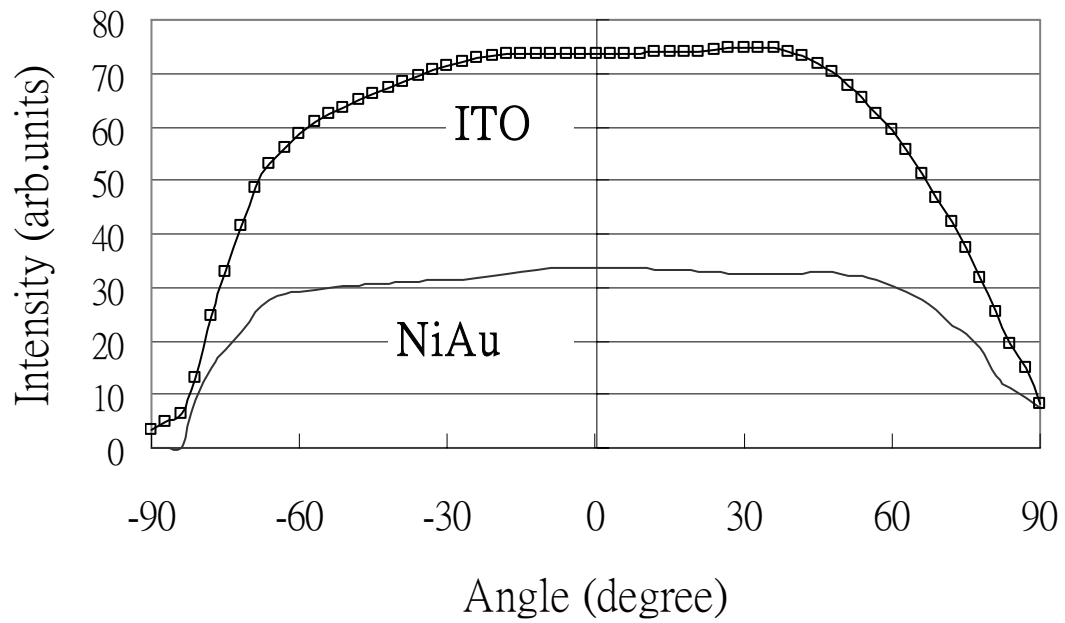


Fig.5-14. Radiation pattern of ITO LED and NiAu LED.

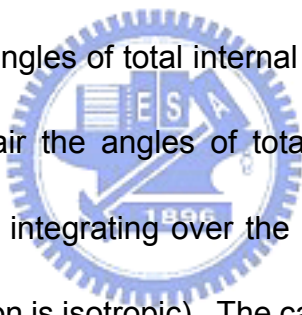
By this figure 5-14 , we also find the larger luminous intensity can be achieved from ITO LED than that of NiAu LED at different emission angle.

Chapter 6. Conclusions

6.1 Conclusions

In light emitting diodes, the spontaneous emission (SE) of photons in directions which are not extracted is highly detrimental to the efficiency of the LED. For general lighting applications the conversion efficiency from electrical energy to useful light energy is an important factor determining whether LEDs may be used to replace conventional lighting technologies.

A straightforward estimate of the amount of light which can be extracted can be obtained by calculating the angles of total internal reflection for light going from GaN (refractive index ~ 2.48) to air the angles of total internal reflection in going from sapphire ($n \sim 1.73$) to air and integrating over the respective solid angles (assuming that the spontaneous emission is isotropic). The calculations are detailed in appendix 1 and tabulated in table 6-1.



Direction of light emission	% of total emission
Top	4.2 %
Bottom (through the substrate)	4.2 %
confined in sapphire substrate ($n=1.73$)	20 %
confined in Guided Layer ($n=2.48$)	71.6 %

Table 6-1 Estimate of light output from top and bottom of LED and percentage confined by total internal reflection in the GaN and the sapphire layers

Thus, in a conventional GaN LED without any coatings or other efficiency enhancing schemes, only about 4.2% of the light is emitted in air towards the top and over 90% of the light is confined by total internal reflection to the GaN and sapphire layers.

In this thesis, we use one dimensional photonic crystal structure to improve the extraction efficiency of GaN LED. The metal reflector is popularly used to increase the light output by reflecting the downward radiation from active layer. The drawback of metal reflector is the a little bit higher reflection loss than the reflector of dielectric materials. This drawback of metal reflector results from the different light reflection mechanism. The photonic crystal structure is a better reflector to enhance the light extraction. We see the axial light output is doubled compared to the sample before the PhC –ODR layers coated (section 5-1). And the wall plug efficiency increases by around 12% when the LED adds photonic crystal reflector (section 5-3). When the photonic crystal reflector LED is applied to the smaller viewing angle lamp packaging, we can see the strong enhancement of axial optical emission (section 5-2). We know the major cost of LEDs is the cost of the epitaxial wafer. If we only have the lower-rank epitaxial wafers, we can use the photonic crystal reflector technology to improve the light extraction efficiency. The radiation quality of this kind LED (PC LED) should be as good as the conventional LED made from the higher-rank epitaxial wafers.

參考文獻

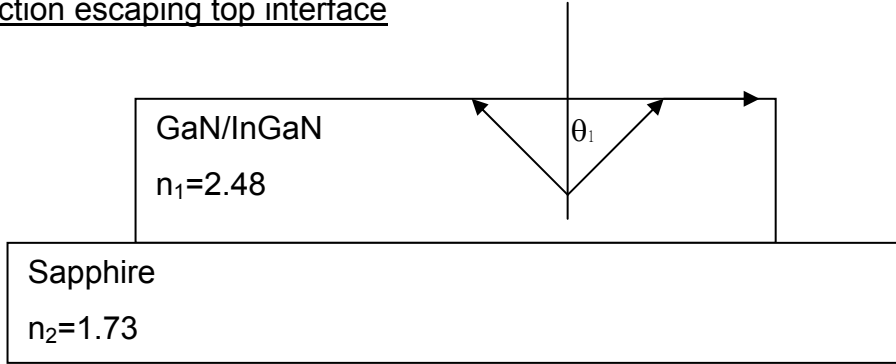
- [1] J.H. Edgar (Ed.), Properties of group-III nitrides, INSPEC, 1994.
- [2] Stacia Keller, Steven P. DenBaars, J. Crystal Growth 248(2003) 479~486
- [3] D.W. Kim *, Y.J. Sung, J.W. Park, G.Y. Yeom, A study of transparent indium tin oxide (ITO) contact to p-GaN, Thin Solid Films 398 –399 (2001) 87–92
- [4] J.M. Delucca, H.S. Venugopalan, S.E. Mohny, R.F. Jr. Karlicek, Appl. Phys. Lett. 73 (23) (1998) 3402.
- [5] J.S. Jang, I.S. Chang, H.K. Kim, T.Y. Seong, S. Lee, S.J. Park, Appl. Phys. Lett. 74 (1) (1999) 70.
- [6] M. Suzuki, T. Arai, T. Kawakami, S. Kobayashi, S. Fujita, Y. Koide, Y. Taga, M. Murakami, J. Appl. Phys. 86 (9) (1999) 5079.
- [7] T. Maragall, O. Buchinsky, D.A. Cohen, A.C. Abare, M. Hansen, S.P. DenBaars, L.A. Coldren, Appl. Phys. Lett. 74 (26) (1999) 3930.
- [8] J.W. Bae, H.J. Kim, J.S. Kim, N.E. Lee, G.Y. Yeom, Vacuum 56 (2000) 77.
- [9] Hyunsoo Kim, Seong-Ju Park, and Hyunsang Hwang, *Member, IEEE*
Design and Fabrication of Highly Efficient GaN-Based Light-Emitting Diodes
IEEE TRANSACTIONS ON ELECTRON DEVICES, VOL. 49, NO. 10,
OCTOBER 2002
- [10] S. Nakamura, T. Mukai, and M. Senoh, “Candela-class high-brightness InGaN/AlGaIn double-heterostructure blue-light-emitting diodes,”
Appl. Phys. Lett., vol. 64, pp. 1687–1689, 1994.
- [11] R. P. Vaudo, I. D. Goepfert, T. D. Moustakas, D. M. Beyea, T. J. Frey, and K. Meehan, “Characteristics of light-emitting diodes based on GaN p-n junctions grown by plasma-assisted molecular beam epitaxy,” *J. Appl. Phys.*, vol. 79, pp. 2779–2783, 1996.

- [12] S. Nakamura and G. Fasol, *The Blue Laser Diode*. Berlin, Germany: Springer, 1997.
- [13] P. Perlin, M. Osinski, P. G. Eliseev, V. A. Smagley, J. Mu, M. Banas, and P. Satori, "Low-temperature study of current and electroluminescence in InGaN/AlGaIn/GaN double-heterostructure blue light-emitting diodes," *Appl. Phys. Lett.*, vol. 69, pp. 1680–1682, 1996.
- [14] I. Mártil, E. Redondo, and A. Ojeda, "Influence of defects on the electrical and optical characteristics of blue light-emitting diodes based on III–V nitrides," *J. Appl. Phys.*, vol. 81, pp. 2442–2444, 1997.
- [15] G.Y. Zhao, G.Yu, T. Egawa, J.Watanabe, T. Jimbo, and M. Umeno, "Energy-gap narrowing in a current injected InGaIn/AlGaIn surface light emitting diode," *Appl. Phys. Lett.*, vol. 71, pp. 2424–2426, 1997.
- [16] Y. Arakawa, T. Someya, and K. Tachibana, "Progress in GaN-based nanostructures for blue light-emitting quantum dot lasers and vertical cavity surface emitting lasers," *IEICE Trans. Electron.*, vol. E83-C, pp. 564–572, 2000.
- [17] H. X. Jiang, S. X. Jin, J. Li, J. Shakya, and J. Y. Lin, "III-nitrides blue microdisplays," *Appl. Phys. Lett.*, vol. 78, pp. 1303–1305, 2001.
- [16] I. Eliashevich, Y. Li, A. Osinsky, C. A. Tran, M. G. Brown, and R. F. Karlicek, Jr., "InGaIn blue light-emitting diodes with optimized n-GaN layer," *Proc. SPIE*, vol. 3621, pp. 28–36, 1999.
- [19] H. Kim, J.-M. Lee, C. Huh, S.-W. Kim, D.-J. Kim, S.-J. Park, and H. Hwang, "Modeling of a GaN-based light-emitting diode for uniform current spreading," *Appl. Phys. Lett.*, vol. 77, pp. 1903–1904, 2000.

- [20] H. Kim, S.-J. Park, and H. Hwang, "Effects of current spreading on the performance of GaN-based light-emitting diodes," *IEEE Trans. Electron Devices*, vol. 48, pp. 1065–1069, 2001.
- [21] J. E. Siewenie and L. He, "Characterization of thin metal films processed at different temperatures," *J. Vac. Sci. Technol. A*, vol. 17, pp. 1799–1804, 1999.
- [22] S. X. Jin, J. Li, J. Y. Lin, and H. X. Jiang, "InGaN/GaN quantum well interconnected microdisk light-emitting diodes," *Appl. Phys. Lett.*, vol. 77, pp. 3236–3238, 2000.
- [23] J. Joannopoulos, R. Meade, and J. Winn, *Photonic Crystals*. Princeton University Press, 1995.
- [24] S. Fan, P. Villeneuve, J. Joannopoulos-JD, and E. Schubert, "High extraction efficiency of spontaneous emission from slabs of photonic crystals," *Physical Review Letters*, vol. 78, Apr. 1997.
- [25] A. Mekis, J. Chen, I. Kurland, S. Fan, P. Villeneuve, and J. Joannopoulos, "High transmission through sharp bends in photonic crystal wave-guides," *Physical Review Letters*, vol. 77, pp. 3787–3790, Oct. 1996.
- [26] E. Yablonovitch, "Photonic band-gap structures," *Journal of the Optical Society of America B*, vol. 10, Feb. 1993.
- [27] C. Anderson and K. Giapis, "Larger two-dimensional photonic band gaps," *Physical Review Letters*, vol. 77, Sept. 1996.
- [28] S. Fan, P. Villeneuve, and J. Joannopoulos, "Large omnidirectional band gaps in metalodielectric photonic crystals," *Physical Review B*, vol. 54, Oct. 1996.

Appendix 1 - Estimate of the fraction of light extracted from GaN LED

Fraction escaping top interface

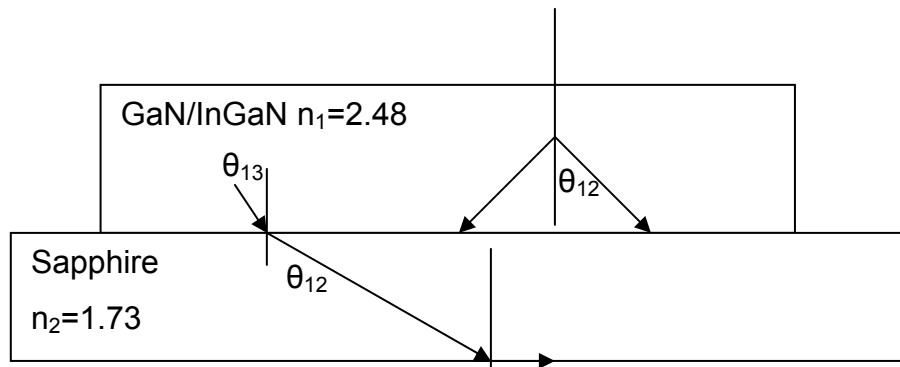


$$\theta_1 = \sin^{-1}(1/2.48) = 0.403 \text{ rad}$$

Only fraction of light which falls within the cone of the critical angle can escape.
Integrating over the unit sphere:

$$\text{Fraction of light escaping top surface} = \frac{\int_0^{\theta_1} 2\pi \sin \theta d\theta}{\int_0^{\pi} 2\pi \sin \theta d\theta} = \frac{[-\cos \theta]_0^{\theta_1}}{[-\cos \theta]_0^{\pi}} = \frac{0.0849}{2} = 0.042$$

Fraction escaping sapphire and fraction confined in the GaN layer



Critical angle at the GaN/Sapphire interface is $\theta_{12} = \sin^{-1}(1.73/2.48) = 0.442$ rad

Critical angle at the Sapphire/air interface is $\theta_{23} = \sin^{-1}(1/1.73) = 0.616$ rad

Angle of incidence in GaN for critical angle in sapphire

$$= \sin^{-1}(1.73/2.48 \times \sin 0.616) = 0.4032$$

Hence fraction escaping sapphire lower surface = 0.042

Fraction (excluding TIR from top surface) escaping GaN/sapphire interface =

$$\frac{\int_0^{\theta_{12}} 2\pi \sin \theta d\theta}{\int_0^{\pi} 2\pi \sin \theta d\theta} = \frac{[-\cos \theta]_0^{\theta_{12}}}{[-\cos \theta]_0^{\pi}} = \frac{0.2835}{2} = 0.1417$$

Hence fraction confined in the GaN waveguide = $1 - 0.1417 - 0.1417 = 0.7165$

Fraction entering sapphire = $0.1417 + \text{TIR from top}$

$$= 0.1417 + (0.1417 - 0.042) = 0.2414$$

Fraction confined in sapphire = $0.2414 - 0.042 = 0.2$